

Understanding Dynamics among Corporate Finance Themes: The Role of Ambiguity and Implementation Delay

Sami Attaoui

Finance Department
NEOMA Business School
1 Rue du Maréchal Juin,
76130 Mont-Saint-Aignan, France
EMAIL: sami.attaoui@neoma-bs.fr
TEL: +33 2 32 82 46 85

Wenbin Cao

Finance Department
NEOMA Business School
1 Rue du Maréchal Juin,
76130 Mont-Saint-Aignan, France
EMAIL: wenbin.cao@neoma-bs.fr
TEL: +33 2 32 82 57 42

Xiaoman Duan

College of Business Administration
Sam Houston State University
1821 Avenue I, Huntsville,
Texas 77341, USA
EMAIL: duan@shsu.edu
TEL: +1-936-294-4149

Sora Kim

Finance Department
NEOMA Business School
1 Rue du Maréchal Juin,
76130 Mont-Saint-Aignan, France
EMAIL: sora.kim@neoma-bs.fr
TEL: +33 2 32 82 57 00

Understanding Dynamics among Corporate Finance Themes: The Role of Ambiguity and Implementation Delay*

Abstract

We develop a real options model that investigates the connections among the five common themes in corporate finance suggested by Graham (2022), incorporating both drift and jump ambiguity, as well as implementation delay. In the context of disinvestment, our analysis reveals that miscalibration leads to conservative policies, particularly in conjunction with a short horizon, which further exacerbates conservatism in decision-making. Additionally, under high ambiguity, ambiguity aversion prompts immediate disinvestment, providing insights into the recent puzzling surge in disinvestment demand.

Key Words— Disinvestment, real option, jump ambiguity, implementation delay.

JEL code— C61, D81, G30, G31.

1 Introduction

Recently, there has been a surge in divestiture/disinvestment. For instance, during the 2020 pandemic shock, Bain & Company (Wininger and Rujana, 2021) reports that “*the crisis has added urgency to divest as companies redirect scarce resources toward the best opportunities amid increasing industry disruption.*” Notably, 40% of nearly 300 surveyed M&A practitioners express a strong demand for disinvestment due to pandemic-induced uncertainty. Additionally, large-sample evidence from Pagano and Zechner (2022) reveals a significant decline in median total assets from 2019 to 2020 for firms in both the United States and Europe. This surge is a surprise because during the same period there has been an increase in risk/uncertainty, and traditional real options modeling would lead to less disinvestment.¹ In this paper, we use a real options framework to explain this puzzling surge. However, rather than relying on traditional modeling assumptions, we instead make assumptions consistent with realistic aspects of real-world corporate finance (as discussed in Graham, 2022).

In his presidential address (Graham, 2022), John R. Graham identifies five recurring themes that highlight the disconnect between academic theories and real-world corporate practices. He advocates revising existing models by incorporating these themes to better align theoretical predictions with actual behavior. The themes include: (1) *Short Horizon*: Firms prioritize near-term goals, often at the expense of long-term value creation; (2) *Miscalibration*: Managers frequently misjudge risks, resulting in suboptimal financial decisions; (3) *Conservative Policy*: Firms adopt overly cautious strategies, often setting hurdle rates well above their actual cost of capital; (4) *Sticky Policy*: Corporate policies are often slow to adjust to evolving conditions due to managerial inertia; and (5) *Simple Decision Rule*: Managers rely on heuristics, such as payback periods, rather than sophisticated theoretical frameworks.

In Table 1, we summarize how our modeling approach addresses the five themes. We first link each theme to specific elements of our model, including its assumptions and predictions, and then discuss the novel implications of our findings. Building on these insights, we explore the connections among the themes, particularly the causal relationship highlighted by Graham (2022), who attributes *Short Horizon* and *Miscalibration* as causes of *Conservative Policy*:

“*How might we expect corporate policies to be designed given that planning is reli-*

¹In this framework, uncertainty is typically modeled using Brownian motion, which follows a normal distribution with a constant and known standard deviation. For a textbook treatment, see Dixit and Pindyck (1994).

able only a couple years out and firms do not anticipate tail risks well? Companies adopt what appear to be conservative policies (the third theme), perhaps in an effort to provide slack in the event downside surprises occur.”

Table 1: Summary of the themes and our modeling approach.

The first column presents the five themes identified by Graham (2022). The second column aligns each theme with our corresponding modeling assumptions or predictions. The third column connects the elements of our model to the original discussions in Graham (2022). The fourth column highlights the novel implications derived from these themes relative to traditional models.

Theme	Model	Mechanism	Novel Implications
<i>Short Horizon</i>	A finite maturity on the disinvestment option.	With a finite horizon, agents doubt reaching the first-best threshold in time.	A shorter maturity reduces the disinvestment option value, aligning the real option threshold with the NPV threshold. → <i>Short Horizon</i> causes <i>Conservative Policy</i> , especially when interacting with <i>Miscalibration</i> or <i>Sticky Policy</i> .
<i>Miscalibration</i>	Risk and ambiguity structures in the asset value dynamics.	Managers miscalibrate one of these uncertainty sources: 1) volatility, jumps, and <i>ex ante</i> skewness 2) drift and jump ambiguity shares.	High ambiguity prompts immediate disinvestment. Concerns about miscalibrating risk and ambiguity structures result in conservative policies. → <i>Miscalibration</i> causes <i>Conservative Policy</i> .
<i>Conservative Policy</i>	High ambiguity about the asset value dynamics.	A smaller information set increases ambiguity. Managers adopt high discount rates in capital budgeting.	In contrast, volatility increases the project value hence lowers the discount rate.

<i>Sticky Policy</i>	Implementation delay in the selling process.	Delay lowers the threshold, as managers expect the asset value to grow to the first-best threshold upon sales completion. Ambiguity amplifies the delay effect.	Delay further reduces the discount rate, while high ambiguity drives firms to commit to immediate disinvestment regardless of other conditions. → When interacting with <i>Miscalibration</i> and <i>Short Horizon</i> , <i>Sticky Policy</i> intensifies policy conservatism.
<i>Simple Decision Rule</i>	High ambiguity + A finite maturity	Ambiguity raises the optimal boundary for disinvestment, leading to convergence toward the NPV threshold.	High ambiguity and short horizons create the perception that managers favor NPV, while they are actually employing real options. → <i>Simple Decision Rule</i> emerges as a consequence of the combined effects of <i>Miscalibration</i> , <i>Short Horizon</i> , and <i>Sticky Policy</i> .

A traditional real options model for disinvestment (e.g., Dixit and Pindyck, 1994; Lambrecht and Myers, 2007) relies on three stylized assumptions: (1) perfectly calibrated uncertainty, (2) instantaneous implementation, and (3) an infinite planning horizon. In this framework, holding an asset generates dividend flows but requires ongoing maintenance costs. Disinvestment occurs when the asset's value drops to a real options threshold (termed the first-best threshold) set below the break-even net present value (NPV) level.

The perfectly calibrated uncertainty assumption models uncertainty as Brownian motion with fixed and known volatility. Under this setup, higher volatility lowers the disinvestment threshold and increases the option value of waiting—discouraging disinvestment. Yet this prediction directly contradicts empirical observations of surging disinvestment during recent periods of elevated volatility.

To reconcile this discrepancy, we use the realistic assumption of *Miscalibration*, modeling managers who face and exhibit aversion to both drift ambiguity (uncertainty over expected growth rates) and jump ambiguity (uncertainty over jump frequency/size).² We demonstrate that immediate disinvestment can be optimal under sufficiently high ambiguity, resolving the empirical puzzle. Our modeling approach aligns with Graham (2022), who attributes miscalibration to managers' inability to anticipate tail events, as seen in their tendency to underestimate extreme outcomes: “25% of firm realizations are below (above) the 10th (90th) percentile of their forecasted distributions.”

To formalize this, we extend the Recursive Multiple Prior Utility (RMPU) framework (Chen and Epstein, 2002) and integrate robust optimization techniques for jump processes (Quenez and Sulem, 2013, 2014).³ In our model, miscalibration arises from two interconnected drivers: the risk structure, characterized by volatility, jumps, and *ex ante* skewness in asset value dynamics, and the ambiguity structure, which differentiates subjective concerns over drift ambiguity and jump ambiguity (Seo, 2009; Baillon et al., 2018).

Our model finds unique effects of ambiguity on disinvestment decisions that contrast with the established literature on irreversible investment. In the context of investment (e.g., Nishimura and Ozaki, 2007; Cao et al., 2022), ambiguity-averse managers are concerned with the worst-case scenario of buying an asset with the least favorable growth rate and positive jump risk. However, the opposite holds true for disinvestment: managers exhibit concern for a scenario in which they prematurely sell an asset that might yield a high growth rate and more positive jumps. This stark contrast leads to a distinct result: ambiguity introduces discontinuity in disinvestment decisions. On the one hand, sufficiently high ambiguity triggers immediate disinvestment. The intuition is as follows: when agents do not know the asset's true value distribution, they fear selling too early and potentially forfeiting high future growth. Concern about this worst-case concern creates a negative ambiguity premium (a penalty), leading to the perception that diminished dividends or even equity injections are necessary as a form of insurance against unfavorable outcomes. When ambiguity is sufficiently high, holding an asset is per-

²Ambiguity (Knightian uncertainty) refers to unknown probability distributions, distinct from risk where distributions are known. Ambiguity aversion reflects a preference for compensation to tolerate this uncertainty (Ellsberg, 1961). We emphasize that although jumps are inherent to the objective state dynamics, ambiguity stems from the agent's subjective beliefs (Seo, 2009; Baillon et al., 2018).

³The RMPU framework generalizes the maxmin preference for ambiguity aversion (Gilboa and Schmeidler, 1989) to continuous time. RMPU models ambiguity as a set of alternative perceived models differing in drift, with ambiguity aversion quantified via compensation requirements.

ceived as costly, eroding retention incentives and prompting immediate disinvestment to resolve ambiguity. On the other hand, moderate ambiguity increases the disinvestment threshold towards the NPV threshold and lowers the disinvestment option value. This stands in marked contrast to irreversible investment decisions, where both volatility and ambiguity increase the cash flow threshold.

The second traditional assumption of instantaneous implementation predicts uniform uncertainty effects on disinvestment across firms with varying characteristics. This assumption, which posits no lag between initiating and finalizing asset sales, disregards significant real-world frictions. Empirical evidence, however, reveals stark contradictions to the traditional framework. Graham (2022) highlights that organizational inertia creates “long lags before changes appear in the data,” even for economically rational decisions. With respect to disinvestment specifically, Ramey and Shapiro (2001) demonstrate that winding down operations can take years due to challenges in asset redeployability. Recent findings (Campello et al., 2021, 2022) further undermine the no-delay assumption: the presence of liquid secondary asset markets attenuates the effect of uncertainty on disinvestment, contradicting the prediction under the instantaneous implementation assumption.

We address these contradictions by incorporating the realistic assumption of *Sticky Policy* through implementation delay—the time lag between initiating and finalizing a sale. We show that ambiguity amplifies the effect of delay on disinvestment, consistent with Campello et al. (2021, 2022), because asset illiquidity is a major cause of delay. Furthermore, ambiguity and delay affect disinvestment and investment decisions (Delaney, 2022) differently—a distinction we will discuss in details in Section 2.4. In our model, delay can postpone disinvestment at a lower threshold than the first-best threshold in a traditional real options model, because managers expect the asset value to grow to the first-best threshold upon sales completion. Ambiguity-averse managers, concerned with the worst-case scenario of selling an asset with the highest growth potential, postpone disinvestment even further. This stems from their perception that the asset’s value may grow more rapidly under ambiguity, inducing them to retain the asset at even lower thresholds. Importantly, while we partially incorporate *Sticky Policy* as an assumption, we later demonstrate how it can emerge endogenously within our model.

Lastly, traditional real options models assume an infinite planning horizon, which generates a constant first-best threshold. This threshold is set below the NPV threshold by an uncertainty multiplier, reflecting the option value. Despite this theoretical prescription, Graham

(2022) highlights that managers in practice typically eschew sophisticated real options methods in favor of simple rules such as payback periods or NPV criteria, creating an apparent disconnect between theory and practice.

Our extension addresses this theoretical-empirical gap by adopting the realistic assumption of *Short Horizon*. We show that a short planning horizon can create the perception that managers favor NPV rules over real options methods. Specifically, by assuming a finite horizon on the disinvestment option, our model exposes managers to hitting time uncertainty—concern about whether the remaining time is sufficient to reach the first-best threshold. This uncertainty produces a non-constant threshold that converges to the NPV threshold as the planning horizon shortens. Consequently, under a short horizon, the real option implied threshold approximates the NPV threshold, creating the observed phenomenon where managers appear to adopt the simple NPV criteria. In this extended analysis, we recognize the lack of analytical solutions and employ the Least-Square Monte Carlo method introduced by Longstaff and Schwartz (2001) for numerical solutions.

Furthermore, our framework incorporating these realistic assumptions yields novel predictions that extend substantially beyond the scope of traditional models under conventional assumptions. Regarding *Conservative Policy* in capital budgeting, Graham (2022) notes that companies often set hurdle rates well above their cost of capital, leading to lower valuations for their projects. In this regard, our model analysis results produce the following testable hypotheses: (1) *Ambiguity and delay independently and jointly increase the discount rate.* Ambiguity and delay each diminish project value, and together amplify this effect; (2) *For industries with the same objective volatility and jump parameters, differences in concerns over drift versus jump ambiguity lead to variations in discount rates.* Managers concerning both sources of ambiguity are particularly prone to apply higher discount rates, aligning with our finding that the disinvestment option value reaches its minimum under the presence of both types of ambiguity; (3) *In industries without ambiguity, delay effects on the discount rate are independent of the objective risk structure. Under ambiguity, this is no longer true.* Ambiguity distorts the mean growth rate, on which the delay effect relies; (4) *In industries without ambiguity, delay effects on the discount rate are independent of ex-ante skewness. Under ambiguity, negative skewness in the return process amplifies the effect of delay.* The worst-case mean growth rate is highest with negative skewness under the reference measure.; and (5) *Short planning horizons increase discount rates and interact with both ambiguity and delay.* Short horizons decrease the disinvestment

option value, and this effect is magnified when both delay and ambiguity exist.

Our results uncover intricate connections among the five themes, suggesting that certain themes can lead to others. As discussed above, *Miscalibration*, *Short Horizon*, and *Sticky Policy* can each result in *Conservative Policy* and create amplified effects when they interact. Furthermore, *Sticky Policy* can arise as a consequence without relying on delay as a cause, as we show that once the ambiguity surpasses a critical threshold, managers will adopt an immediate disinvestment policy, irrespective of delay. Additionally, *Miscalibration* and *Short Horizon* each can lead to *Simple Decision Rule* and also produce amplified effects through their interaction.

Our results under moderate ambiguity offer a coherent explanation for recent empirical observations. Several studies (Jens, 2017; Carvalho, 2018; Campello et al., 2021, 2022) report substantial decreases in disinvestment attributed to heightened uncertainty, but they do not differentiate between risk structure and ambiguity structure. Hence, future empirical research should investigate our testable implications summarized above. Jens (2017) highlights that economic policy uncertainty has a pronounced effect on the disinvestment activities of small firms and those in politically sensitive industries, even after controlling for cash flow volatility. Additionally, Humphery-Jenner et al. (2019) emphasize that disinvestment experience enhances its efficiency. Given that small firms and sensitive industries often face higher ambiguity, and that experience can mitigate ambiguity—viewed as a form of learning under ambiguity (Epstein and Schneider, 2007), our model aligns with these empirical findings.

This paper is the first to provide comprehensive explanations on the interconnections among all five corporate finance themes proposed by Graham (2022). While prior research has addressed specific themes, this study integrates them into a unified model, highlighting their relationships. For example, Dessaint et al. (2023) suggest that a decline in the reliability of investors' long-term signals may deter firms from pursuing long-term investments (*Short Horizon*). In another facet, DeAngelo (2022) argues that managers' insufficient knowledge contributes to failures in capital structure decisions (*Miscalibration*). On the topic of *Conservative Policy*, Geelen et al. (2024) demonstrate that firms with longer-lived assets adopt more conservative financing strategies, while Barry et al. (2022) find that firms with lower corporate flexibility tend to postpone or reduce capital spending. Regarding *Sticky Policy*, Fukui et al. (2024) reveal that firms' nominal costs of capital are sticky relative to inflation, limiting the effectiveness of monetary policy in spurring investment. In addition, Charoenwong et al. (2024) show that firms face difficulties in promptly adjusting their investments to productivity shocks due to the constraints

imposed by pre-planned capital budgets. Lastly, contrary to textbook theories of NPV maximization, Ben-David and Chinco (2023) assert that managers prioritize maximizing earnings-per-share (EPS) as a unified framework for a wide array of corporate decisions (*Simple Decision Rule*).

Additionally, our paper bridges two strands of real options literature: one studying ambiguity effects and another exploring the delay effects. Earlier real options models addressing ambiguity primarily fall under the drift ambiguity framework, focusing predominantly on irreversible investment. Notable examples include Nishimura and Ozaki (2007), Thijssen (2011), Miao and Wang (2011), Cheng and Riedel (2013), and Flor and Hesel (2015), among others. A recent contribution is Cao et al. (2022), who explore joint investment and financing decisions under jump ambiguity.⁴ Real options models explicitly addressing disinvestment, particularly considering the role of ambiguity, remain scarce. Notable examples in this realm include Alvarez and Stenbacka (2006) and Lambrecht and Myers (2007).

Lastly, earlier real options models incorporating delay primarily focus on Brownian risk, as seen in the works of Bar-Ilan and Strange (1996), Alvarez and Keppo (2002), Tsyplakov (2008), Thijssen (2010), Sarkar and Zhang (2013, 2015), and Jeon (2021). Thijssen (2015) explores the effects of jump risks and delay; however, he does not consider the role of ambiguity. Delaney (2021) introduces market incompleteness in the context of irreversible investment under delay problem. Delaney (2022) investigates the combined effect of ambiguity and delay on irreversible investment. Several key distinctions set our work apart. First, Delaney (2022) focuses solely on drift ambiguity. Secondly, worst-case scenarios differ, resulting in value functions that exhibit reverse monotonicity to the state variable in ours and Delaney (2022). Third, in Delaney (2022), the impact of delay on the investment boundary varies depending on the level of ambiguity because ambiguity distorts the drift toward the negative domain. In our study, however, ambiguity dominates delay in the context of disinvestment; it is optimal to divest immediately under sufficiently high ambiguity, irrespective of delay. In other words, the delay impact is significant only under moderate ambiguity. Finally, we also explore the role of a finite decision horizon.

⁴Li and Wang (2023) study irreversible investment under jump ambiguity, assuming a normally distributed jump size. They characterize ambiguity aversion using the variational preference framework of Maccheroni et al. (2006), where the worst-case scenario is moderated by an entropy penalty, making it less extreme than under RMPU. For further discussions on the worst-case scenario under the variational preference framework, particularly in the context of drift ambiguity, one can refer to Miao and Rivera (2016).

2 Theoretical results

2.1 Baseline

2.1.1 Disinvestment

We adopt the standard real options model in Lambrecht and Myers (2007) to study disinvestment. At time 0, an agent possesses an asset, whose value is characterized by a stochastic process denoted as $X(t) := X(t, \omega)$. This process is defined on a probability space (Ω, \mathcal{F}, Q) , equipped with a standard complete filtration $\mathbf{F} := \{\mathcal{F}_t | t \geq 0\}$. While holding the asset, the agent continuously collects dividends at a constant rate of $\iota \geq 0$, where the amount collected during the time interval $[t, t + dt]$ is $\iota X(t) dt$.⁵ The agent also incurs a constant cost of holding the asset at a rate of $C > 0$ per unit of time, which can be interpreted as the maintenance cost. Consequently, the instantaneous net cash flow to the agent is given by $\iota X(t) dt - C dt$. The agent chooses to disinvest when the accumulated net cash flow falls below a certain threshold. Without loss of generality, we assume the agent realizes no proceeds from asset liquidation.⁶

Given the stochastic nature of $X(t)$, the agent may not find it optimal to sell when $\iota X(t) - C < 0$ right away, as there is the potential for $X(t)$ to rebound later. Anticipating the possibility of this rebound, the agent may choose to inject capital to cover the cost C , until either $\iota X(t) - C \geq 0$ or $X(t)$ falls to a sufficiently low level X^* , representing the optimal disinvestment boundary. At this boundary, the value of postponing the decision no longer outweighs the cost. In this context, the agent can be seen as possessing an American put option on the asset.

Specifically, we define Q as the risk-neutral probability measure, where $X(t)$ follows a geometric Lévy process described by:

$$\frac{dX(t)}{X(t^-)} = \mu dt + \sigma dW(t) + \int_{\mathbb{R}} (e^u - 1) \tilde{N}(dt, du), \quad \mu = r - \iota \geq 0, \quad X(0) = x > 0, \quad (1)$$

where $\sigma > 0$, and $r > 0$ (the risk-free rate) are constants. The parameter μ is the risk-neutral asset growth rate after dividends.⁷ This specification simplifies expressions and allows for a more

⁵Since our focus is on disinvestment decisions, we treat ι as exogenous. Future work could explore optimizing ι as a control policy.

⁶This assumption implies that the fixed cost C is the primary driver of disinvestment. However, this assumption is not restrictive, as our main results still hold if the agent recovers a fraction $\alpha \in (0, 1)$ of the asset value upon sale. Results under this alternative assumption are available upon request.

⁷We implicitly assume $\iota \in (0, r]$ under the risk-neutral measure, a common assumption in dividend models, as

concise presentation. In Equation (1), $W(t)$ is a standard Brownian motion, and $\tilde{N}(dt, du) = N(dt, du) - \nu(du)dt$ is a compensated Poisson random measure. The Lévy measure is denoted as $\nu(du) := \mathbb{E}[N(1, du)]$ and characterizes the jump component of the process.

For reasons that will be elaborated on, we specify the jump component as a compound Poisson process with intensity $\lambda < +\infty$ and a double exponential distribution for the jump size, resulting in a double exponential jump-diffusion process, first introduced by Kou (2002).⁸ This specification is as follows:

$$\nu(du) = \lambda f(du), \tag{2}$$

where $f(du)$ is a probability density function that combines positive and negative jumps. It comprises two parts: $p\eta_1 e^{-\eta_1 u} \mathbf{1}_{u \geq 0}$ for positive jumps and $q\eta_2 e^{\eta_2 u} \mathbf{1}_{u < 0}$ for negative jumps, where $\eta_1 > 1$, $\eta_2 > 0$, $p, q \geq 0$, and $p + q = 1$.

The model specification exhibits noteworthy advantages. Firstly, it enables the explicit characterization of positive and negative surprises by controlling the log conditional mean positive and negative jump sizes. This feature serves as a starting point to address *Miscalibration*. Secondly, as demonstrated by Kou and Wang (2004), the model provides analytical solutions for valuing American-style perpetual options. We analyze the optimal policy in an infinite horizon, where disinvestment resembles a perpetual American put, enabling tractable valuation. The model's treatment of positive and negative jumps accommodates diverse prior assumptions, key to our study of ambiguity.

2.1.2 Implementation delay

Graham (2022) views *Sticky Policy* as a manifestation of “inertia” in the decision-making process, with one strand of literature highlighting that such inertia leads to implementation delays in disinvestment. Thywissen et al. (2017) conduct detailed surveys on five Western European multi-business firms and find that the disinvestment decision-making process can extend up to 57 months. They interpret these findings through the lens of “organizational inertia,” as described by Hannan and Freeman (1977, 1984), which relates to limitations on organizations’ ability to adapt and their relatively slow responses to environmental threats or opportunities.

seen in Décamps et al. (2011) and Bolton et al. (2011).

⁸Due to the jump part, the market is incomplete and thus the conventional riskless hedging cannot be achieved. But one can still construct a stochastic discount factor process in a rational expectations equilibrium with a representative agent and obtain an implied risk-neutral measure, see Kou (2002).

Contributing factors include cognitive biases among decision-makers, political deadlock, the sunk cost fallacy, and institutional barriers to change. Additionally, Sandri et al. (2010) provide experimental evidence of pronounced “psychological inertia” in the disinvestment decision-making process, indicating that individuals tend to hold on to losing projects longer than real-options reasoning would predict.

Another strand of literature highlights asset redeployability or liquidity as key to an effective selling process. Ramey and Shapiro (2001) highlight that winding down operations and selling equipment can take several years, underscoring the sectoral specificity of capital. Firms often incur significant costs related to search and matching to address this specificity and cope with market thinness. Kim and Kung (2017) additionally suggest that the financial constraints of potential buyers can affect the efficiency of asset sales. Moreover, they point out the role of industrial organization, as firms that liquidate assets due to operational and financial challenges may precipitate similar difficulties for industry peers. Given the sector-specific nature of assets, this industrial effect can contribute to further delays in implementation.

To incorporate implementation delay, we follow the standard approach commonly employed in the investment literature (e.g., Bar-Ilan and Strange, 1996; Alvarez and Keppo, 2002). In our scenario, the agent initiates the selling process at a random (stopping) time $\tau \in [0, T]$, where $T \leq +\infty$, but the collection of payoff proceeds occurs at $\tau + \delta$, with $\delta > 0$ representing the constant implementation delay. As a result of the implementation delay, *payoff uncertainty* emerges, as the sale initiates at τ based on the unknown asset value at $\tau + \delta$. During the interval $[\tau, \tau + \delta]$, the agent still holds the asset and incurs maintenance costs.

Our assumption regarding the independence between uncertainty and implementation delay is in line with empirical evidence. For instance, Kim and Kung (2017) show that industries with the most redeployable assets include leather, tobacco, and chemical manufacturing (their Table 1). At the opposite end of the spectrum, industries with the least redeployable assets include textile, pulp, and apparel manufacturing. It is clear that the industries at the two ends of the spectrum do not exhibit significantly different levels of cash flow uncertainty. Since assets redeployability is a key determinant of implementation delay, their findings reinforce the validity of our assumption.

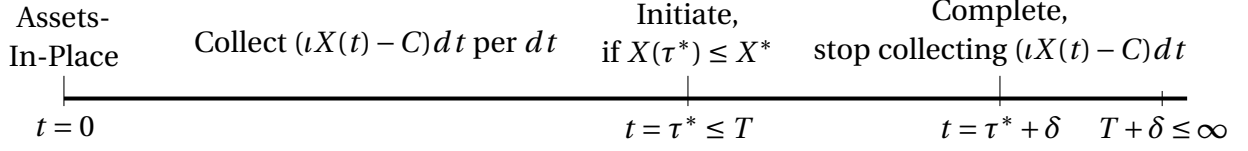


Figure 1: Timeline for disinvestment of assets-in-place under implementation delay

2.1.3 Disinvestment under implementation delay

With the presence of implementation delay and under an infinite time horizon, the agent solves the following optimal stopping problem for profit maximization

$$\begin{aligned}
 V(0) &= \sup_{\tau} \mathbb{E}_0 \left[\int_0^{\tau+\delta} e^{-rt} (\iota X(t) - C) dt \right] = \mathbb{E}_0 \left[\int_0^{\tau^*+\delta} e^{-rt} ((r - \mu) X(t) - C) dt \right] \\
 &= \mathbb{E}_0 \left[X(0) - \frac{C}{r} + e^{-r(\tau^*+\delta)} \left(\frac{C}{r} - X(\tau^* + \delta) \right) \right].
 \end{aligned} \tag{3}$$

where $\tau \in [0, +\infty]$ is a \mathcal{F}_0 -stopping time and we have used the relation $\iota = r - \mu$ defined before. The first line in (3) signifies that the agent selects the optimal stopping time τ^* for disinvestment initiation. At $\tau^* + \delta$, the process completes, and the agent ceases to receive the net payout stream generated by holding the asset, denoted as $\iota X(t) - C$. Figure 1 illustrates the process. Within this context, the agent faces payoff uncertainty during $[\tau^*, \tau^* + \delta]$.

The second line follows from the Dynkin formula and offers an alternative interpretation. If it is never optimal to sell ($\tau^* = +\infty$), the value of holding is the current asset value $X(0)$, reduced by the perpetual maintenance cost C/r . If it is optimal to sell at a finite time ($\tau^* < +\infty$), the agent will recover the (perpetual) maintenance cost stream C/r at $\tau^* + \delta$ and relinquish the asset valued at $X(\tau^* + \delta)$. Clearly, for $\tau^* < +\infty$, optimality implies a positive selling proceeds of $C/r - \mathbb{E}_{\tau^*}[X(\tau^* + \delta)] > 0$. Here, the conditional expectation with respect to \mathcal{F}_{τ^*} underscores that the decision to stop at time τ^* is made based on the expectation of $X(\tau^* + \delta)$ using the information available at τ^* . In other words, the agent lacks information about $X(t)$ for $t \in [\tau^*, \tau^* + \delta]$ at the time of the decision.

2.2 Introducing ambiguity

2.2.1 The belief set

To study jump ambiguity, we expand the Chen and Epstein (2002) utility framework, accommodating uncertain jump intensity and size distribution (Lévy measure). We utilize the general results from Quenez and Sulem (2013, 2014), who provide the comparison theorem for backward stochastic differential equations (BSDEs) under Lévy process and general results for related optimal stopping problems under ambiguity.

Let Θ denote the set of density generators. Each density generator $\theta \in \Theta$ is binary, i.e., $\theta = (\theta_W, \theta_N)$, where θ_W is for the Brownian motion and θ_N is for the Poisson random measure. For each density generator $\theta \in \Theta$, let $Z^\theta(t)$ be the solution of the (forward) SDE:

$$dZ^\theta(t) = Z^\theta(t^-) \left(-\theta_W(t) dW(t) - \int_{\mathbb{R}} \theta_N(t, u) d\tilde{N}(dt, du) \right), \quad t \in [0, T], \quad Z^\theta(0) = 1.$$

For $\theta_W(t)$, we adopt the κ -ignorance specification of Chen and Epstein (2002), i.e., $\theta_W(t) \in [-\kappa, \kappa]$, $0 < \kappa < \infty$. Based on the technical requirement in Quenez and Sulem (2013, 2014), we use the following specification for $\theta_N(t, u)$:

$$\begin{aligned} \theta_N(t, u) &= 1 - e^{\theta_{N,1}(t)u} \mathbf{1}_{u \geq 0} - e^{\theta_{N,2}(t)u} \mathbf{1}_{u < 0}, \\ \theta_{N,1}(t) &\in [-M_1, 0], \quad \theta_{N,2}(t) \in [0, M_2], \quad \text{and} \quad M_1, M_2 > 0. \end{aligned}$$

Our specification for $\theta_N(t, u)$ follows the jump size distribution in Equation (2). As shown below, under the worst-case measure, the additivity of the two exponential terms leads to distortions to the positive jump component and to the negative jump component respectively.

To construct the set of priors, we define a probability measure Q^θ on \mathcal{F}_T equivalent to Q^0 for $\theta \in \Theta$ as

$$\mathbb{E}^\theta[\mathbf{1}_A] = \mathbb{E}[\mathbf{1}_A Z_T^\theta], \quad A \in \mathcal{F}_T.$$

Hence, we have under Q^θ

$$dW^\theta(t) = dW(t) + \theta_W(t) dt$$

being a Brownian motion and

$$\tilde{N}^\theta(dt, du) = \tilde{N}(dt, du) + \theta_N(t, u) \nu(du) dt = N(dt, du) - (1 - \theta_N(t, u)) \nu(du) dt \quad (4)$$

being a compensated Poisson random measure by Girsanov's theorem.⁹ Taken together, under Q^θ , $X(t)$ is given by

$$\frac{dX(t)}{X(t^-)} = \left(\mu - \theta_W(t)\sigma - \int_{\mathbb{R}} (e^u - 1)\theta_N(t, u)\nu(du) \right) dt + \sigma dW^\theta(t) + \int_{\mathbb{R}} (e^u - 1)\tilde{N}^\theta(dt, du).$$

Our method of distorting the reference measure can attenuate the unconditional impact of positive or negative jumps, depending on the monotonicity of the decision maker's value function relative to the state variable. The term "unconditional" indicates that the distortion to the jump intensity is endogenously determined. This will become clearer when we discuss the worst-case scenario in Section 2.3.1.

Equation (4) indicates that $N^\theta(dt, du)$ has a Lévy measure $\nu^\theta(du) = (1 - \theta_N(t, u))\nu(du)$ under Q^θ . We can express $\nu^\theta(du)$ as

$$\nu^\theta(du) = \lambda_t^\theta f_t^\theta(du),$$

where λ_t^θ is the distorted jump intensity given by

$$\lambda_t^\theta = \lambda \int_{\mathbb{R}} (1 - \theta_N(t, u)) f_u du = \lambda \left(\frac{p\eta_1}{\eta_1 - \theta_{N,1}(t)} + \frac{q\eta_2}{\eta_2 + \theta_{N,2}(t)} \right),$$

and the distorted jump size density is given by

$$\begin{aligned} f_{u,t}^\theta &= \frac{(1 - \theta_N(t, u)) f_u}{\int_{\mathbb{R}} (1 - \theta_N(t, u)) f_u du} \\ &= p_t^\theta (\eta_1 - \theta_{N,1}(t)) e^{-(\eta_1 - \theta_{N,1}(t))u} \mathbf{1}_{u \geq 0} + q_t^\theta (\eta_2 + \theta_{N,2}(t)) e^{(\eta_2 + \theta_{N,2}(t))u} \mathbf{1}_{u < 0}, \end{aligned}$$

with p_t^θ and q_t^θ being the distorted probabilities of upward and downward jumps given by

$$p_t^\theta = \frac{p\eta_1(\eta_2 + \theta_{N,2}(t))}{p\eta_1(\eta_2 + \theta_{N,2}(t)) + q\eta_2(\eta_1 - \theta_{N,1}(t))} \text{ and } q_t^\theta = \frac{q\eta_2(\eta_1 - \theta_{N,1}(t))}{p\eta_1(\eta_2 + \theta_{N,2}(t)) + q\eta_2(\eta_1 - \theta_{N,1}(t))}.$$

Table 2 summarizes the Lévy measures for $N^\theta(dt, du)$ for the set of priors specified $\theta_{N,1}(t) \in [-M_1, 0]$ and $\theta_{N,2}(t) \in [0, M_2]$.

[Insert Table 2 about here]

⁹See, for example, Chapter 1.4 of Øksendal and Sulem (2019).

2.2.2 Calibrating ambiguity structure

In our model, the inclusion of both diffusion and jumps poses two challenges for the agent in terms of calibration. The first challenge is to calibrate the relative contribution of diffusion versus jumps in total return variation and *ex ante* skewness under a given probability measure, which we refer to as risk structure calibration. The second challenge is to calibrate the total amount of ambiguity deemed plausible and the relative concern over diffusion ambiguity versus jump ambiguity under the worst-case measure, a task we refer to as ambiguity structure calibration. While the literature offers alternative ways to address the first challenge both parametrically (e.g., Eraker et al., 2003) and non-parametrically (e.g., Aït-Sahalia and Jacod, 2012), addressing the second challenge is complex, as it requires identifying alternative models the agent finds plausible given historical asset value data.

To address the second challenge, we employ relative entropy and detection-error probabilities advocated by Anderson et al. (2003). Relative entropy and detection-error probabilities gauge ambiguity by comparing likelihoods from an alternative model (Q^θ) to those from the reference model (Q^0). When small deviations exist between the alternative and reference models, distinguishing between them through trajectory observation becomes difficult. Conversely, significant deviations result in distinguishable trajectories, simplifying differentiation. Therefore, accurately quantifying the extent of ambiguity involves considering a set of alternative models that are statistically indistinguishable from the reference model.

Relative entropy measures the distance between a pair of probability measures. Given an alternative measure Q^θ and the reference measure Q^0 , we can write the growth in entropy of Q^θ relative to Q^0 over the time interval $[t, t + \Delta t]$ as

$$G(t, t + \Delta t) = \mathbb{E}_t^\theta \left[\ln \left(\frac{Z^\theta(t + \Delta t)}{Z^\theta(t)} \right) \right], \quad \mathcal{R}(\theta_t) = \lim_{\Delta t \rightarrow 0} \frac{G(t, t + \Delta t)}{\Delta t} \quad t \geq 0.$$

Similar to Drechsler (2013) and Aït-Sahalia and Matthys (2019), we characterize the set of admissible models as

$$\left\{ \theta(t) = (\theta_W(t), \theta_N(t)) \mid \mathcal{R}(\theta(t)) \leq h, \text{ for } t, h \geq 0 \right\},$$

where the constant h defines an upper bound on the set of alternative models. As h approaches zero, the set of alternative models shrinks, implying that the agent is confident in the reference model. By contrast, a larger h indicates that the agent is willing to consider a wider set of models

that are statistically farther away from the reference model, suggesting more room for ambiguity. Throughout the paper, we refer to h the total amount of ambiguity under consideration.

Next, the independence of the diffusion and jump components (*per* Itô-Lévy Decomposition) implies that the two components contribute to relative entropy growth in an additive way, or equivalently $\mathcal{R}(\theta(t)) = \mathcal{R}(\theta_W(t)) + \mathcal{R}(\theta_N(t))$. We use h_W and h_N satisfying $h_W + h_N = h$ to regulate contributions of drift ambiguity and jump ambiguity to total relative entropy.

The key to disciplining the extent of ambiguity is the determination of h . Anderson et al. (2003) provide a likelihood-based approach, detection-error probability, to quantify the amount of ambiguity that seems plausible to the agent. Let $\zeta^\theta(t) = \ln(Z^\theta(t))$ denote the log of the Radon-Nikodym derivative process. Intuitively, if an alternative model Q^θ is substantially different from the reference model Q^0 , it would be straightforward for the agent to detect the difference by assessing log-likelihoods given finite samples of data. Formally, the detection-error probability is defined as (assuming an equal prior on Q^θ and Q^0)

$$\pi(t, T; h) = \frac{1}{2} \left[Q^0 \left\{ \zeta^\theta(T) > 0 \mid \mathcal{F}_t \right\} + Q^\theta \left\{ \zeta^\theta(T) < 0 \mid \mathcal{F}_t \right\} \right]. \quad (5)$$

The first term inside the bracket on the right-hand side denotes the probability that an agent will falsely reject the correct model Q^0 in favor of Q^θ when a history of the state process with length $T - t$ is generated under Q^0 . Conversely, the second term is the probability that an agent will erroneously reject the correct model Q^θ in favor of Q^0 when a history of the state process with length $T - t$ is generated under Q^θ . Further insight into the computation of the detection-error probability can be found in Section 3.2.

2.3 Disinvestment under ambiguity and delay

2.3.1 Characterizing the worst-case measure

With the set of priors constructed and determined above, we can state the general disinvestment problem under delay and ambiguity as

$$V(0, \tau^*, \theta^*) = \sup_{\tau \in \mathcal{T}_{0,T}} \inf_{Q^\theta} \mathbb{E}_0^\theta \left[X(0) - \frac{C}{r} + e^{-r(\tau+\delta)} \left(\frac{C}{r} - X(\tau+\delta) \right) \right], \quad \text{for } T \leq +\infty, \quad (6)$$

where $\mathcal{T}_{0,T}$ is the set of stopping times taking values in $[0, T]$. Using Lemma 1 in the Internet Appendix, we can evaluate $V(0, \tau^*, \theta^*)$ by first finding the minimum expectation measure Q^{θ^*} for an arbitrary τ . Then, we can solve the optimal stopping problem under Q^{θ^*} .

The following Proposition characterizes the worst-case scenario for the agent.

Proposition 1. *The density generator that gives the minimum expectation in (6) is $\theta^* = (\theta_W^*, \theta_N^*) = (-\kappa, 1 - \mathbf{1}_{u \geq 0} - e^{M_2 u} \mathbf{1}_{u < 0})$ for all $t \in [0, \tau + \delta]$.*

An immediate implication of the above is that under Q^{θ^*} , $X(t)$ follows

$$dX(t)/X(t^-) = \mu^* dt + \sigma dW^{\theta^*}(t) + \int_{\mathbb{R}} (e^u - 1) \tilde{N}^{\theta^*}(dt, du) \quad (7)$$

where

$$\begin{aligned} \mu^* &= \mu + \kappa\sigma + \int_{\mathbb{R}} (e^u - 1)(1 - \mathbf{1}_{u \geq 0} - e^{M_2 u} \mathbf{1}_{u < 0}) \nu(du) \\ &= \mu + \underbrace{\kappa\sigma}_{\text{Drift Ambiguity}>0} + \underbrace{\lambda q \left(\frac{1}{(\eta_2 + 1)} - \frac{\eta_2}{(\eta_2 + M_2 + 1)(\eta_2 + M_2)} \right)}_{\text{Jump Ambiguity}>0}. \end{aligned} \quad (8)$$

Equation (8) indicates that under the worst-case measure, the drift is distorted upward by $\kappa\sigma + \lambda q / (\eta_2 + 1) - \lambda q \eta_2 / ((\eta_2 + M_2 + 1)(\eta_2 + M_2))$, where the first (second) term is due to drift (jump) ambiguity.

The drift ambiguity distortion, $\kappa\sigma$, is consistent with previous studies. Cheng and Riedel (2013) provide the general results for optimal stopping under drift ambiguity. In particular, they show that when a perpetual American option exercise payoff is monotonically decreasing in the state variable, the worst-case measure is characterized with the upward adjustment by $\kappa\sigma$ to the drift, and vice versa. From Equation (6), it is clear that the disinvestment payoff is decreasing in the state variable.

Before delving into the detailed discussion of $X(t)$ under Q^{θ^*} , it's important to highlight that jump ambiguity distortions remain independent of drift ambiguity. This property arises from the independence of the Brownian term and the jump term in line with the Itô-Lévy Decomposition. In essence, both drift ambiguity and jump ambiguity can coexist, or only one type may manifest, depending on the decision maker's varying concern for each ambiguity form. This dynamic becomes clearer as we delve into the calibration of detection-error probabilities in Section 3.2.

Significantly, aside from reducing drift, jump ambiguity introduces additional distortions in jump intensity and size distribution. For instance, the magnitude of the conditional mean for negative jumps (in log units) reaches its minimum in absolute value at $-1/\eta_2^*$, where $\eta_2^* = \eta_2 + M_2$, while the magnitude for positive jumps (in log units) attains its maximum at $1/\eta_1^*$, with $\eta_1^* = \eta_1$. The conditional probability of positive jumps reaches its maximum at $p^* = p(\eta_2 + M_2)/(p(\eta_2 + M_2) + q\eta_2)$, and the conditional probability of negative jumps achieves its minimum at $q^* = q\eta_2/(p(\eta_2 + M_2) + q\eta_2)$. The jump intensity suggested by the worst-case scenario isn't the highest or lowest, but instead equals $\lambda^* = \lambda(p + q\eta_2/(\eta_2 + M_2))$. More details regarding the range of these parameters under the worst-case measure Q^{θ^*} can be found in Table 2.

The interpretations are based on the premise that the firm's disinvestment payoff decreases with the asset value dynamics. Consequently, in the worst-case scenario, positive jumps have the highest probability and mean magnitude, while negative jumps have the lowest probability and mean magnitude. The jump intensity falls in an intermediate range because the firm anticipates the highest possible arrival rate of positive jumps and the lowest possible arrival rate of negative jumps.

This behavior of jump intensity reflects the “unconditional” nature discussed below Equation (4). For instance, in the extreme case $p = 0$, there are no positive jumps, and the jump intensity λ_t lies within the range $[\lambda\eta_2/(\eta_2 + M_2), \lambda]$, with λ^* attaining the minimal value $\lambda\eta_2/(\eta_2 + M_2)$ per Table 2. This implies that when only negative jumps occur, their mean arrival rate is the lowest possible. Conversely, when there are no negative jumps ($p = 1$), the jump intensity $\lambda_t = \lambda^* = \lambda$, representing the highest possible mean arrival rate. Therefore, when both positive and negative jumps are present, the mean arrival rate of a jump falls between these two extremes.

The expression for $X(t)$ under Q^{θ^*} further reveals that jump ambiguity distorts the entire distribution of $X(t)$ while drift ambiguity only distorts the mean. This is evident by examining the moment generating function of $Y(t) = \ln X(t)$ as

$$\mathbb{E}^{\theta^*} [e^{\nu Y(t)}] = e^{t\phi^{\theta^*}(\nu)}, \quad (9)$$

where

$$\phi^{\theta^*}(\nu) = \frac{1}{2}\sigma^2\nu^2 + \left(\mu^* - \frac{1}{2}\sigma^2 - \lambda^* \left(\frac{p\eta_1^*}{\eta_1^* - 1} + \frac{q^*\eta_2^*}{\eta_2^* + 1} - 1\right)\right)\nu + \lambda^* \left(\frac{p^*\eta_1^*}{\eta_1^* - \nu} + \frac{q^*\eta_2^*}{\eta_2^* + \nu} - 1\right).$$

It is immediate that the variance of $Y(t)$ is

$$\mathbb{E}^{\theta^*} [(Y(t) - \mathbb{E}^{\theta^*} [Y(t)])^2] = \sigma^2 t + 2\lambda^* \left(\frac{p^*}{(\eta_1^*)^2} + \frac{q^*}{(\eta_2^*)^2} \right) t.$$

Jump ambiguity notably impacts the variance of $Y(t)$, a distinction from scenarios where only drift ambiguity is at play—since κ exclusively appears in μ^* . Further insight into how jump ambiguity shapes the distribution of $Y(t)$ is explored in Section 3.2, where we numerically compute its first four central moments.

2.3.2 Optimal immediate disinvestment under high ambiguity

After finding the worst-case measure, we start to solve for the optimal disinvestment policy and value function. Under the worst-case measure, so long as $Q^{\theta^*} \{\tau^* < +\infty\} = 1$, we have

$$\begin{aligned} V^\infty(0, \tau^*, \theta^*) &= \sup_{\tau \geq 0} \mathbb{E}_0^{\theta^*} \left[X(0) - \frac{C}{r} + e^{-r(\tau+\delta)} \left(\frac{C}{r} - X(\tau+\delta) \right) \right] \\ &= \lim_{T \rightarrow \infty} \sup_{\tau \in [0, T]} \mathbb{E}_0^{\theta^*} \left[X(0) - \frac{C}{r} + e^{-r(\tau+\delta)} \left(\frac{C}{r} - X(\tau+\delta) \right) \right]. \end{aligned} \quad (10)$$

Unlike the irreversible investment problem, where the optimal stopping time is nonzero irrespective of ambiguity, it is possible for (10) to have an optimal stopping time equal to zero.

Proposition 2. *Let $\eta_2^* = \eta_2 + M_2$. If the following inequality holds*

$$\mu^* = \mu + \kappa\sigma + \left(\frac{\lambda q}{(\eta_2 + 1)} - \frac{\lambda q \eta_2}{(\eta_2^* + 1)\eta_2^*} \right) \geq r, \quad (11)$$

then $\tau^ = 0$. Furthermore, the continuation region D for $r = \mu^*$ is the empty set \emptyset , and for $r < \mu^*$ is of the form*

$$D = (-\infty, x^*), \quad \text{with} \quad x^* < \frac{C}{e^{\mu^* \delta} (r - \mu^*)}.$$

Proposition 2 suggests that with high ambiguity, the agent resolves it early by exercising the disinvestment option without waiting. This holds regardless of the implementation delay δ .¹⁰ This highlights that in disinvestment, ambiguity outweighs implementation delay considerations, unlike in investment (see Section 2.4).

¹⁰Without delay, prior studies in other contexts also show early resolution of ambiguity (e.g., Nishimura and Ozaki, 2004; Miao and Wang, 2011; Attaoui et al., 2021).

To interpret Proposition 2, we can use the Dynkin's formula to rewrite the value function under the worst-case measure in Equation (10) as

$$V^\infty(0, \tau^*, \theta^*) = \sup_{\tau \geq 0} \mathbb{E}_0^{\theta^*} \left[\int_0^{\tau+\delta} ((r - \mu^*)X(t) - C) dt \right] = \sup_{\tau \geq 0} \mathbb{E}_0^{\theta^*} \left[\int_0^{\tau+\delta} (\iota^* X(t) - C) dt \right],$$

where the perceived total payout under ambiguity is

$$\iota^* = r - \mu^* = \iota + \underbrace{\left[-\kappa\sigma - \left(\frac{\lambda q}{(\eta_2 + 1)} - \frac{\lambda q \eta_2}{(\eta_2^* + 1)\eta_2^*} \right) \right]}_{\text{Negative Ambiguity Premium}}, \quad (12)$$

and ι denotes the dividend yield in the absence of ambiguity as in Section 2.1. Consequently, if the condition specified in Equation (11) is met, we observe that $\iota^* < 0$, indicating that the ambiguity-averse agent perceives that retaining the asset would result in negative dividends. These perceived negative dividends are a result of the agent's demand for a sufficiently high negative ambiguity premium, as detailed in Equation (12). As a result, the agent lacks any motivation to keep the asset at any point in time, as doing so would yield strictly negative perceived cash flows, ultimately resulting in negative position values. In Section 3.2, we demonstrate that the condition in Equation (11) can be satisfied under realistic scenarios. The presence of a negative ambiguity premium aligns with *Conservative Policy*, as it implies a reduction in payouts through various mechanisms. In Section 3.5, we illustrate the empirical implications.

Proposition 2 introduces a notable feature: a discontinuity in the continuation region concerning ambiguity level. The continuation region comprises asset value levels where postponing disinvestment is optimal. Under moderate ambiguity, this region is represented as $(X^*, +\infty)$, as elucidated in Proposition 3. In practical terms, once the asset value falls to or below X^* from above, it becomes optimal to disinvest. However, as the ambiguity level increases and reaches the critical point satisfying the equality in Equation (11), the optimal disinvestment threshold ceases to exist. This implies that, for any asset value, postponing disinvestment is worse than stopping immediately. Furthermore, if the ambiguity level rises beyond the critical point, meeting the inequality in Equation (11), the continuation region becomes impractical because asset value cannot be negative. This discontinuity will be instrumental in our discussions in Section 3.4.

2.3.3 The joint impact of ambiguity and delay under low ambiguity

In the scenario where the agent exhibits lower ambiguity aversion, resulting in the inequality (11) not being satisfied, the agent will find it optimal to disinvest at a later time.

Proposition 3. *Let $\eta_1^* = \eta_1$ and $\eta_2^* = \eta_2 + M_2$. If the inequality (11) does not hold, then the infinite horizon value function $V^\infty(0, \tau^*, \theta^*)$ as in (10) has the following solution*

$$\begin{aligned} V^\infty(0, \tau^*, \theta^*) \\ = x - \frac{C}{r} + e^{-r\delta} \frac{C}{r} \left[d_{1,0} \left(\frac{X^*}{x} \right)^{\beta_3} + d_{2,0} \left(\frac{X^*}{x} \right)^{\beta_4} \right] - e^{(\mu^* - r)\delta} X^* \left[d_{1,1} \left(\frac{X^*}{x} \right)^{\beta_3} + d_{2,1} \left(\frac{X^*}{x} \right)^{\beta_4} \right], \end{aligned} \quad (13)$$

where

$$\tau^* = \inf_t \{X(t) \leq X^*\}, \quad X^* = \underbrace{e^{-\mu^* \delta}}_{\text{Delay Multiplier} < 1} \underbrace{\frac{\beta_3 \beta_4 (\eta_2^* + 1)}{(\beta_3 + 1)(\beta_4 + 1) \eta_2^*}}_{\text{Uncertainty Multiplier} < 1} \underbrace{\frac{C}{r}}_{\text{NPV Threshold}}, \quad X(0) = x. \quad (14)$$

Here $\beta_1, \beta_2, \beta_3, \beta_4$ satisfying $-\infty < -\beta_4 < -\eta_2^* < -\beta_3 < 0 < \beta_1 < \eta_1^* < \beta_2 < \infty$, are the four roots of the equation $G(\beta) = r$, with

$$G(\beta) = \frac{1}{2} \sigma^2 \beta^2 + \left[\mu^* - \frac{1}{2} \sigma^2 - \lambda^* \left(\frac{p^* \eta_1^*}{\eta_1^* - 1} + \frac{q^* \eta_2^*}{\eta_2^* + 1} - 1 \right) \right] \beta + \lambda^* \left(\frac{p^* \eta_1^*}{\eta_1^* - \beta} + \frac{q^* \eta_2^*}{\eta_2^* + \beta} - 1 \right), \quad (15)$$

where

$$\begin{aligned} \mu^* &= \mu + \kappa \sigma + \lambda q \left(\frac{1}{(\eta_2 + 1)} - \frac{\eta_2}{(\eta_2^* + 1) \eta_2^*} \right), \quad \lambda^* = \lambda (p + q \eta_2 / \eta_2^*), \\ p^* &= \frac{p \eta_2^*}{p \eta_2^* + q \eta_2}, \quad q^* = \frac{q \eta_2}{p \eta_2^* + q \eta_2}, \quad d_{1,0} = \frac{\eta_2^* - \beta_3 \beta_4}{\beta_4 - \beta_3 \eta_2^*}, \\ d_{2,0} &= \frac{\beta_4 - \eta_2^* \beta_3}{\beta_4 - \beta_3 \eta_2^*}, \quad d_{1,1} = \frac{\eta_2^* - \beta_3 \beta_4 + 1}{\beta_4 - \beta_3 \eta_2^* + 1}, \quad d_{2,1} = \frac{\beta_4 - \eta_2^* \beta_3 + 1}{\beta_4 - \beta_3 \eta_2^* + 1}. \end{aligned} \quad (16)$$

For brevity, we limit the discussions on the mathematical expressions in Proposition 3 and refer back to them when we interpret our numerical analysis results. Equation (14) shows that both ambiguity and delay influence the disinvestment boundary X^* , with the effect of delay depending on the level of ambiguity. The term C/r represents the myopic NPV boundary, where divesting breaks even. The ‘‘Uncertainty Multiplier’’ captures the combined effects of risk and

ambiguity, considering contributions from both diffusion and jumps. This multiplier, being less than one, reflects the option value of delaying disinvestment to a lower threshold.

The “Delay Multiplier” demonstrates that delay lowers the boundary by incorporating an expected growth mechanism. When we apply the Delay Multiplier to both sides of Equation (14), the right-hand side becomes the optimal boundary without delay. Since $\mu^* > \mu \geq 0$, delay further reduces the disinvestment boundary due to expected growth during the delay period. Furthermore, the delay effect on the value function is stronger than on the boundary, because the value function is further lowered by the factors $e^{-\mu^* \delta \beta_3} (< 1)$ and $e^{-\mu^* \delta \beta_4} (< 1)$, according to Equation (13).

When delay is absent ($\delta = 0$), jump ambiguity M_2 increases the boundary and the Uncertainty Multiplier, lowering the disinvestment option value. Although calculating $\partial X^* / \partial M_2$ is technically complex, we can infer the effect of M_2 from the inequality

$$\frac{\beta_3}{\beta_3 + 1} \frac{C}{r} < X^* < \frac{\beta_4}{\beta_4 + 1} \frac{C}{r}.$$

As both β_3 and β_4 increase with M_2 , the lower and upper bounds for X^* rise, leading to an overall increase in X^* as M_2 grows. However, the elevated boundary does not necessarily imply a shorter expected disinvestment time, as the state process has greater upward potential under the worst-case measure.

Therefore, to facilitate our analysis, we introduce another critical quantity known as the Arrow-Debreu (AD) price of disinvestment, denoted as $AD = \mathbb{E}_0^\theta[e^{-r\tau}]$. Here, τ represents a (random) disinvestment time, and the AD price signifies the present value of one dollar received at the disinvestment time τ . In cases without ambiguity, where the agent has a single prior, a lower disinvestment boundary equates to a longer hitting time and thus a lower AD price, provided that the state process level is currently within the continuation region. However, under ambiguity, when comparing the boundaries in the reference and worst-case measures, we can no longer infer the expected hitting time, as the state process has distinct parameters under the two measures. Therefore, it becomes necessary to examine the AD price separately. Additionally, when studying disinvestment within finite horizons, the disinvestment boundary becomes a function of the remaining time to maturity, making it more convenient to examine the AD price.

2.4 Compare disinvestment with investment

Our results in Section 2.3 highlight that ambiguity and delay can affect disinvestment and investment in distinct ways. Delaney (2022) examines the investment problem under drift ambiguity and delay. She shows that the project value process has the lowest possible drift under the worst-case measure. Implementation delay can either decrease or increase the optimal investment boundary, depending on the level of ambiguity. The interpretation of this result also follows that the delay effect on the investment boundary is through the Delay Multiplier $e^{-\mu^*\delta}$. Unlike in our disinvestment case, where ambiguity increases μ^* , in the investment case, ambiguity lowers μ^* . Therefore, the worst-case μ^* can switch its sign from positive to negative as ambiguity increases. As a result, delay decreases (increases) the boundary for the low (high) level of ambiguity. In contrast, delay lowers the disinvestment boundary only for a moderate level of ambiguity because a high level of ambiguity leads to immediate disinvestment irrespective of the delay. In this spirit, ambiguity and delay play equal roles in influencing investment, while ambiguity dominates delay in determining disinvestment.

3 Model implications

In Section 3.1, we discuss our parameter choices. Section 3.2 details the calibration of total ambiguity and ambiguity structure. In Section 3.3, we present our baseline results. Section 3.4 covers the comparative statics analysis. Section 3.5 elaborates on the connections among the five themes identified by Graham (2022) and how our results provide a coherent explanation of recent empirical evidence.

3.1 Parameter choices

Table 3, Panel A, presents the parameter values. A key challenge is specifying the jump parameters, which we base on the jump parameterization of Chen and Kou (2009). They analyze optimal capital structure using a double-exponential jump diffusion process for asset value. To enhance empirical relevance, we align the jump parameters with estimates from prior literature.

Under the risk-neutral measure Q^0 , we set the jump arrival rate parameter $\lambda = 1$, consistent with estimates from index option prices (e.g., Bakshi et al., 1997). We assume equal conditional

probabilities for positive and negative jumps ($p = q = 0.5$). In the baseline, we set equal mean jump sizes for positive and negative jumps ($1/\eta_1 = 1/\eta_2 = 1/7$), resulting in a symmetric *ex ante* log process $Y(t) = \ln(X(t))$ (denoted as $Skew^0$ in Table 3). This symmetry helps illustrate how ambiguity aversion introduces asymmetry in $Y(t)$ under the worst-case scenario.

To account for the documented dispersion in risk-neutral skewness of individual stock returns (Conrad et al., 2013), we also explore two asymmetric reference specifications by adjusting the jump size parameters: $Skew^-$ and $Skew^+$ in Table 3. For $Skew^-$ ($Skew^+$), we increase the mean size of negative (positive) jumps $1/\eta_2$ ($1/\eta_1$) to $1/4$, while keeping the other at the baseline value.

We set other parameters following traditional capital structure models (e.g., Leland, 1998; Goldstein et al., 2001; Strebulaev, 2007; Morellec et al., 2012), because the state process in these models are firm asset value/cash flow under the risk neutral measure. The mean growth rate parameter $\mu = 0.02$, implying a total payout rate $\iota = r - \mu = 0.03$ under the reference measure. The diffusion volatility parameter σ is 0.2. Lastly, we set the risk-free rate $r = 0.05$, the maintenance cost $C = 1$, and the initial project value $x = 20$, indicating that the project value comprises only the option value as the perpetual value $x - C/r = 0$ according to Equation (13).

[Insert Table 3 about here]

In Panel B, we compute the first four central moments of $Y(t)$ using Equations (17) to (20) for our three *ex ante* skewness scenarios at $t = 1$. The negative mean values of $Y(t)$ in all cases result from the Itô formula, specifically due to the exponential martingale correction terms. In the baseline setting ($Skew^0$), the variance is approximately 0.08, indicating a nearly equal contribution from diffusion increments and jumps, given $\sigma^2 = 0.04$. This equal contribution setting ensures a balanced consideration of both increments without biasing the importance of either. Comparing $Skew^-$ and $Skew^+$ reveals interesting observations. Both scenarios exhibit the same variance, skewness (in absolute value), and kurtosis but differ in mean. It is interesting to see that the mean of $Y(t)$ is the smallest under $Skew^+$. But, this result can be reconciled by the mean expression, Equation (17). Notably, skewness and kurtosis values are comparable with the sample median values reported by Conrad et al. (2013).

$$\text{Mean (CM}_1\text{): } \mathbb{E}[Y(t)] = \left[\mu - \frac{1}{2}\sigma^2 + \lambda \left(1 + \frac{p}{\eta_1} - \frac{q}{\eta_2} - \frac{p\eta_1}{\eta_1 - 1} - \frac{q\eta_2}{\eta_2 + 1} \right) \right] t. \quad (17)$$

$$\text{Variance } (CM_2): \mathbb{E}\left[\left(Y(t) - \mathbb{E}[Y(t)]\right)^2\right] = \sigma^2 t + 2\lambda\left(\frac{p}{\eta_1^2} + \frac{q}{\eta_2^2}\right)t. \quad (18)$$

$$\text{Skewness } (CM_3): \mathbb{E}\left[\left(Y(t) - \mathbb{E}[Y(t)]\right)^3\right] / CM_2^{3/2} = 6\lambda t\left(\frac{p}{\eta_1^3} - \frac{q}{\eta_2^3}\right) / CM_2^{3/2}. \quad (19)$$

$$\begin{aligned} \text{Kurtosis } (CM_4): \mathbb{E}\left[\left(Y(t) - \mathbb{E}[Y(t)]\right)^4\right] / CM_2^2 = \\ \left(3\sigma^4 t^2 + \frac{12\lambda^2 p^2 t^2 + 24\lambda p t}{\eta_1^4} + \frac{12\lambda^2 q^2 t^2 + 24\lambda q t}{\eta_2^4} + \frac{24\lambda^2 p q t^2}{\eta_1^2 \eta_2^2} + \frac{12\lambda p \sigma^2 t^2}{\eta_1^2} + \frac{12\lambda q \sigma^2 t^2}{\eta_2^2}\right) / CM_2^2. \end{aligned} \quad (20)$$

3.2 Quantifying ambiguity

We quantify the maximal amount of total ambiguity $h = h_W + h_N$ to characterize the asset value dynamics under the worst-case measure. For the double exponential jump-diffusion process, we can derive the relative entropy growth $\mathcal{R}(Z^{\theta^*}(t))$ as (see the Internet Appendix for the derivations)

$$\mathcal{R}(Z^{\theta^*}(t)) = \frac{1}{2}\kappa^2 + \lambda q \eta_2 \left(\frac{1}{\eta_2} - \frac{2}{\eta_2 + M_2} + \frac{1}{\eta_2 + 2M_2} \right) - \lambda^* q^* \eta_2^* \left(\frac{M_2}{(\eta_2^*)^2} - \frac{1}{\eta_2^*} + \frac{1}{\eta_2^* + M_2} \right), \quad (21)$$

where λ^* , q^* , and η_2^* are the same as in Proposition 3. Under the worst-case measure, the relative entropy growth is $\mathcal{R}(Z^{\theta^*}(t)) = h$. Moreover, given that the diffusion and jump components contribute to relative entropy growth in an additive way, we must have

$$\frac{1}{2}\kappa^2 = h_W,$$

and

$$\lambda q \eta_2 \left(\frac{1}{\eta_2} - \frac{2}{\eta_2 + M_2} + \frac{1}{\eta_2 + 2M_2} \right) - \lambda^* q^* \eta_2^* \left(\frac{M_2}{(\eta_2^*)^2} - \frac{1}{\eta_2^*} + \frac{1}{\eta_2^* + M_2} \right) = h_N.$$

As such we can recover values of κ and M_2 based on h_W and h_N .¹¹

To find the upper bound of h , we follow Anderson et al. (2003) and set h such that the detection-error probability is 10%.¹² For the detection-error probability in (5), Ait-Sahalia and

¹¹Ait-Sahalia and Matthys (2019) provide a formal treatment for the recovery of the ambiguity parameters based on relative entropy growth.

¹²Notably, if this probability is 0.5 (0), the two models become statistically indistinguishable (perfectly distinguishable). A 10% probability corresponds to rejecting one of the models being true at the ten-percent confidence

Matthys (2019) provide a way to calculate it based on the conditional Fourier transform of $\zeta^{\theta^*}(t) = \ln(Z^{\theta^*}(t))$. Given a sample of length $n > 0$, the detection-error probability is

$$\begin{aligned} \pi(t, n; h) &= \frac{1}{2} \left[Q^0 \left\{ \zeta^{\theta^*}(n) > 0 \middle| \mathcal{F}_t \right\} + Q^{\theta^*} \left\{ \zeta^{\theta^*}(n) < 0 \middle| \mathcal{F}_t \right\} \right], \quad t \geq 0, n = mT \\ &= \frac{1}{2} - \frac{1}{2\pi} \int_0^\infty \left(\Re \left[\frac{\phi_{\theta^*}(u, t, n)}{iu} \right] - \Re \left[\frac{\phi_0(u, t, n)}{iu} \right] \right) du. \end{aligned} \quad (22)$$

In the first line, T is the number of years, and m is the sampling frequency, provided that we use annualized parameter values. In the second line, $i = \sqrt{-1}$, $\Re(\cdot)$ denotes the real part of a complex number, and the two conditional Fourier transforms are

$$\phi_0(u, t, n) = \mathbb{E}_t^{Q^0} [e^{iu\zeta^{\theta^*}(n)}], \quad \text{and} \quad \phi_{\theta^*}(u, t, n) = \mathbb{E}_t^{Q^{\theta^*}} [e^{iu\zeta^{\theta^*}(n)}].$$

To implement calibration, we specify h_W/h and $n = mT$. In the baseline scenario, we set $h_W/h = 0.5$, reflecting equal consideration for diffusion and jump ambiguity. For the sample length, we assume a dataset spanning sixty years ($T = 60$), which is reasonable given the availability of CRSP data dating back to the 1920s. Considering sampling frequency, we explore both quarterly ($m = 4$) and monthly ($m = 12$) frequencies. The former represents access to quarterly Compustat data, while the latter allows us to observe the effects of reduced ambiguity with a larger sample size.

3.3 Disinvestment under ambiguity and implementation delay: Baseline

Figure 2 illustrates the detection-error probability calibration results for the two calibration samples. The computed probabilities, denoted as $\pi(n; h)$, are presented as a function of the total relative entropy growth bound h for $h \in [0, h^*]$, where h^* is defined such that $\pi(n; h^*) = 0.1$. The red solid (blue dotted) line represents the quarterly (monthly) sample. The value of h^* calibrated at a quarterly frequency is approximately three times that of the monthly frequency. This reflects the fact that the threefold increase in observations in the monthly sample compared to the quarterly sample reduces the perceived total ambiguity by a factor of three.

[Insert Figure 2 about here]

level. Importantly, the specific value of the detection-error probability does not qualitatively affect our results. If we set it to 5%, the total ambiguity h would increase.

We report the calibrated key parameter values under Q^{θ^*} at h^* in Table 4 Panel A. The following result is immediate.

Proposition 4. *When total ambiguity h^* is calibrated with 60 years of quarterly data, it is optimal to disinvest immediately.*

This result arises from the fact that $\mu^* = 0.059$ under Q^{θ^*} –Quarter, which is greater than $r = 0.05$. Therefore, Proposition 2 indicates the optimal disinvestment time $\tau^* = 0$, signifying immediate disinvestment. In the context of the five themes, this result shows that greater ambiguity encourages both *Sticky Policy* and *Conservative Policy*, as decision-makers prioritize maintaining flexibility and avoiding costly mistakes. Conversely, Proposition 2 does not hold for monthly data, as $\mu^* < 0.05$. Hence, in our subsequent analysis, we focus on the lower level of ambiguity, calibrated using monthly data.

[Insert Table 4 about here]

The calibration results in Panel A align with the insights discussed in Section 2.3.1 regarding the distinctive impact of jump ambiguity in reshaping the entire distribution of $Y(t)$. To illustrate this, we compare the first four central moments of $Y(t)$ under Q^{θ^*} with those under Q^0 in Table 3. Under Q^{θ^*} , mean and skewness increase, while variance and kurtosis decrease. These changes are more pronounced when calibrating ambiguity with quarterly data. Figure 3 provides a probability density plot for the jump size, visually highlighting this shift. Notably, changes in variance and higher moments arise uniquely under jump ambiguity, as numerically demonstrated in Table 5 in our comparative statics analysis.

[Insert Figure 3 about here]

Panel B presents baseline disinvestment results under ambiguity and implementation delay, with ambiguity calibrated using monthly data. We report the optimal disinvestment boundary X^* , AD price of disinvestment $\mathbb{E}_0^{\theta^*} [e^{-r\tau^*}]$, and project value V^* under no delay ($\delta = 0$) and a delay ($\delta = 3$). We also provide the percentage change in optimal quantities due to delay. For instance, -5.82% for X^* under Q^0 represents the change in X^* when δ increases from 0 to 3. To visualize the combined effects of ambiguity and delay, we plot these three quantities against total ambiguity $h \in [0, h^*]$ and delay $\delta \in [0, 3]$ in Figure 4.

[Insert Figure 4 about here]

The results in Panel B offer numerical illustrations for our analytical discussions regarding the ambiguity and delay effects, placed after Proposition 3. Indeed, disinvestment takes place at a higher threshold under ambiguity (Q^{θ^*}). Nevertheless, the higher threshold does not lead to earlier disinvestment, as indicated by the smaller AD price. The higher threshold results in a smaller project value. Furthermore, the delay effect is stronger under ambiguity, and the delay effect on the project value is stronger than on the threshold.

To better interpret our numerical results, we first illustrate the tradeoff in determining the optimal threshold in the absence of delay. Managers aim to maximize the present value of the disinvestment payoff, the stopped perpetual maintenance cost flow's value (C/r) less the abandoned asset value at the future time τ ($X(\tau)$). Although the payoff is maximized when the asset value drops to zero, it can take a long time for this to happen, leading to a small present value. Consequently, managers chooses a lowest possible threshold, balancing the expected time to reach it, and resulting in the maximum discounted payoff. Hence, the optimal threshold is a tradeoff between the *payoff* and the *present value*.

The moments of the state process determine the expected time to reach any threshold with the first moment playing the dominant role. The expected growth (μ) is 0.02 under the reference measure (Table 3) and 0.043 (μ^*) under the worst-case measure (Panel A). Hence, a higher growth rate slows the value decrease. Additionally, under the worst-case measure, the variance is smaller, and the right tail becomes fatter. Collectively, managers perceive a longer expected time for the asset value to drop to any level under ambiguity, explaining the higher threshold and lower project value under ambiguity.

These findings highlight the critical roles of ambiguity and delay in capital budgeting decisions. Our analysis shows that ambiguity and delay independently affect both the disinvestment threshold and project valuation (or discount rate), with their combined impact being more significant than their individual effects. Our results implies that *Miscalibration* leads to *Simple Decision Rule*, because ambiguity increases the disinvestment threshold towards the NPV threshold. Our results also suggests that *Miscalibration* results in *Conservative Policy*, because managers apply a higher discount rate to value the project under ambiguity.

3.4 Comparative statics

3.4.1 Ambiguity structure

In our baseline specification, where the agent places equal concern for drift and jump ambiguity, we proceed to examine the consequences of miscalibrating one of the ambiguity sources. We investigate two cases: $h_W/h \in \{0, 1\}$, representing 0% and 100% concern for drift ambiguity, respectively. Similar to our baseline, we characterize worst-case probability measures Q^{θ^*} by calibrating detection-error probabilities based on the monthly data for the two ambiguity share specifications. Calibration results are reported in Table 5 Panel A, and disinvestment quantities are presented in Panel B. For comparison, we include baseline results from Table 4.

[Insert Table 5 about here]

The total ambiguity level h^* is highest (lowest) when drift (jump) ambiguity is the sole concern. This result is interpreted through the mechanism of detection-error probability calibration. Intuitively, the agent aims to reject models whose sample paths deviate significantly from those generated by the reference model based on historical realizations. Since jumps are rare and extreme events, identifying “outliers” is less challenging with sufficient historical data. Hence, when jump ambiguity is the sole concern, the agent considers a narrower range of alternative models who differ primarily in the jump component. Conversely, as emphasized by Merton (1980), estimating mean return is notoriously difficult. With drift ambiguity as the sole concern, the agent considers a wider range of alternative models who differ in the drift only.

A noteworthy observation from Panel A is that drift ambiguity solely affects the mean of $Y(t)$. For instance, when $h_W/h = 1$, the variance, skewness, and kurtosis of $Y(t)$ under Q^{θ^*} match those under Q^0 in Table 3. Only the mean changes from -0.021 under Q^0 to 0.002 under Q^{θ^*} . However, this is not the case when $h_W/h < 1$. These findings offer numerical illustrations of our analytical discussions in Section 2.3.1 concerning the unique implications of jump ambiguity.

The results in Panel B indicate that the presence of both types of ambiguity results in the highest threshold, the latest disinvestment, the smallest project value, and the strongest delay impacts. This result is consistent with the moments of the state process under these three scenarios. The worst-case growth rate under $h_W/h = 0$, 0.031, is much smaller than under the other two scenarios, 0.043. This result is due to two reasons. First, jump ambiguity distorts the entire

distribution, while drift ambiguity only distorts the expected growth. Second, total ambiguity is lower when jump ambiguity is the only concern (Panel A). Although the return distribution is more tilted to the right under $h_W/h = 0$, the growth rate effect dominates, leading to the lowest threshold, the highest AD price, and the highest project value. Next, the differences in the higher moments explain the results under $h_W/h = 0.5$ and $h_W/h = 1$. The reduced variance and thickened right tail explain why the threshold is higher under $h_W/h = 0.5$.

The results in Panel B offer additional insights regarding the causal relations between *Miscalibration* and *Conservative Policy*. Managers adopt the most conservative policies when they cannot rule out the presence of each type of ambiguity. Consequently, they apply the highest discount rate resulting in the lowest project valuation.

3.4.2 Variance structure and ambiguity structure

In our baseline specification, where diffusion volatility and jumps contribute equally to return variance, we now explore the consequences of miscalibrating one of the risk sources. We consider two scenarios where diffusion volatility contributes to the minority and majority of the return variance under the reference measure while maintaining the same overall variance level. We examine two alternative σ values, 0.15 and 0.25. For each σ value, we adjust the mean jump size parameter $\eta_1 = \eta_2 = \eta$ to match the baseline variance of $Y(t)$ at 0.081, as presented in Table 3. By maintaining the variance, we can systematically evaluate the implications of miscalibrating the variance structure.

Table 6 Panel A displays the results of the variance-matching exercise. The adjusted η values are 5.856 (10.450) for $\sigma = 0.15$ (0.25), indicating an increased (decreased) log mean jump size relative to the baseline. Notably, the kurtosis value is significantly larger for $\sigma = 0.15$, reflecting the heightened importance of jump risk in this scenario.

[Insert Table 6 about here]

Panel B presents the results of the detection-error probability calibration. Notably, the total ambiguity h^* and drift ambiguity κ^* remain unchanged across the two variance structures since σ does not affect relative entropy growth (see Equation 21). The jump ambiguity level M_2^* does differ between the two variance scenarios due to variations in the η parameter, as shown in Panel A. The distortion to (log mean) negative jump size is stronger when the jump size is larger,

as seen in the shift from 1/5.586 to 1/6.459 versus 1/10.450 to 1/11.524. This result indicates that jump ambiguity penalize negative jumps more when jump risk is higher.

The key parameter, μ^* , varies narrowly for $\sigma = 0.15$ and broadly for $\sigma = 0.25$ across h_W/h columns. μ^* is smallest at $h_W/h = 0$ in both cases, yet μ^* is the largest at $h_W/h = 0.5$ for $\sigma = 0.15$ and $h_W/h = 1$ for $\sigma = 0.25$. As discussed in Section 3.4.1, total ambiguity (h^*) is the smallest (largest) when jump (drift) ambiguity is the only concern. When $\sigma = 0.15(0.25)$, jumps play a major (minor) role, and jump ambiguity distorts $\mu = 0.02$ under Q^0 to $\mu^* = 0.032(0.027)$ under Q^{θ^*} , as seen in the columns for $h_W/h = 0$. In contrast, although drift ambiguity (κ^*) remains constant across σ values, its distortion effect ($\kappa^* \sigma$) is stronger for $\sigma = 0.25$, explaining the difference between 0.049 and 0.037 in the $h_W/h = 1$ columns.

The patterns for μ^* are not surprising, as drift ambiguity affects only the drift by design. Higher-moment comparisons confirm this: when jump ambiguity is absent ($h_W/h = 0$), return variance is 0.081 for both σ values. However, variance becomes the smallest (0.073) when jump ambiguity is the sole concern ($h_W/h = 1$) for $\sigma = 0.15$. Additionally, distortions to skewness and kurtosis are more pronounced for $\sigma = 0.15$, reinforcing the stronger effect of jump ambiguity on higher moments when jumps dominate.

The patterns for μ^* explain the ambiguity effect in Panel C. When $\sigma = 0.15$, the threshold is the highest for $h_W/h = 0.5$, leading to the lowest project value and AD price. Notably, as jump risk plays the major role in this case, jump ambiguity alone ($h_W/h = 0$) and drift ambiguity alone ($h_W/h = 1$) affect disinvestment similarly, evidenced by the close thresholds in these two scenarios. In contrast, when volatility plays the major role ($\sigma = 0.25$), drift ambiguity has the strongest negative impact on disinvestment, evidenced by the highest threshold under $h_W/h = 1$.

A key result in Panel C is that the variance structure interacts with delay to impact the disinvestment boundary only when ambiguity is present. In scenarios without ambiguity (Q^0), delay consistently decreases the boundary by 5.82% for both variance structures. This aligns with the fact that the delay multiplier, in the absence of ambiguity, is identical for both scenarios. Under ambiguity, the delay effect on the boundary corresponds to the pattern observed in Panel B for μ^* .

The most crucial finding from Panel C is that ambiguity amplifies the repercussions of miscalibrating the variance structure and the impact of delay on the AD price and project value. In the absence of ambiguity, a miscalibrated variance structure—whether it underestimates or

overestimates the significance of volatility or jumps—has minimal effects on the AD price and project value.

The results in Panel B offer additional insights regarding the causal relations between *Miscalibration* and *Conservative Policy*. If a manager is certain that volatility is the main source of risk in her firm, she can ignore jump ambiguity because drift ambiguity leads to the most adverse valuation scenario. In contrast, she cannot ignore either types of ambiguity, because doing so result in over estimated project value and underestimated delay effect.

3.4.3 *Ex ante* skewness

In our baseline specification, where the return process is symmetric, we now investigate the implications of miscalibrating the *ex ante* risk-neutral skewness. Notably, evidence show that skewness can be positive or negative (Conrad et al., 2013) or even stochastic (e.g., Chabi-Yo, 2012), adding complexity to skewness calibration under the reference measure. We examine the $Skew^-$ and $Skew^+$ specifications from Table 3. Detection-error probability calibration results are presented in Table 7 Panel A, with disinvestment outcomes reported in Panel B. We set $h_W/h = 0.5$ under monthly data.

[Insert Table 7 about here]

The calibration results in Panel A provide insights into the interpretation of disinvestment outcomes in Panel B. The total ambiguity level h^* and drift ambiguity κ^* are identical between both scenarios, because the two scenarios represent reversed jump size distributions. However, since the worst-case scenario for disinvestment penalizes the mean negative jump size, the change in mean negative jump size is more pronounced for $Skew^-$ (decreasing from 1/4 to 1/4.319) than for $Skew^+$ (decreasing from 1/7 to 1/7.559).

The ambiguity effects in Panel B are consistent with the the μ^* values in Panel A. The ambiguity effect is stronger under $Skew^-$, evidenced by the significantly increased threshold, compared to $Skew^+$. This result follows the higher μ^* of 0.048 under $Skew^-$ than 0.043 under $Skew^+$. The μ^* result is consistent with a more significant change in η_2 , resulting in a more significant reduction in the thickness of the left tail.

Similar to the case of variance structure, the delay effect does not depend on *ex ante* skewness in the absence of ambiguity, but not so under ambiguity. the delay effect is stronger under

$Skew^-$, consistent with the higher μ^* value in this case. This result demonstrates that miscalibrating *ex ante* skewness can lead to erroneously estimated delay effect when ambiguity is present.

The results in Panel B offer further insights regarding the causal relations between *Miscalibration* and *Conservative Policy*. Miscalibrating *ex ante* skewness can even result in erroneous disinvestment decisions in the absence of ambiguity. Ambiguity further amplifies the consequences of miscalibration. Moreover, the significant effect of *ex ante* skewness on project value should offer insights into the finding that risk-neutral skewness explains the cross-section of stock returns, as documented by Conrad et al. (2013).

3.4.4 Short planning horizons

In our baseline specification, where the planning horizon is infinite, we proceed to study the effect of *Short Horizon*. We aim to show that delay further accentuates the material impacts that the planning horizon can have on disinvestment decisions. Intuitively, the interaction between delay and planning horizon holds particular significance within the real options context. Traditional irreversible investment/disinvestment models within the real options framework are typically designed for an infinite horizon and lack consideration of delay. In such models, agents adhere to a threshold policy, implying that they will invest/disinvest once the state process (e.g., asset value) hits the threshold for the first time from below (above). Given the infinite planning horizon, the corresponding optimal threshold remains constant, termed the first-best threshold.

As the planning horizon becomes finite, agents grapple with *hitting time uncertainty*—the uncertainty about whether the remaining time is sufficient for the state process to reach the first-best threshold from its current position. The significance of hitting time uncertainty increases as the remaining time approaches zero, prompting the agent to converge toward the NPV rule. This suggests *Short Horizon* results in *Simple Decision Rule*. Hence, the horizon becomes pivotal in delineating the extent of hitting time uncertainty. Conversely, delay introduces payoff uncertainty, with longer delays resulting in heightened uncertainty regarding the payoff. Therefore, in finite horizon problems, the impact of delay might depend on the relative difference between the delay and planning horizon. Notably, the delay effect should be more pronounced when the planning horizon is shorter.

We introduce a terminal period $T < \infty$ for the disinvestment option, indicating that the

firm can only divest its assets until time T . Clearly, within the interval $t \in [0, T]$, the firm opts for a sale only if the asset value falls sufficiently below the present value of the maintenance cost C/r . Hence, the disinvestment option resembles a finite-maturity American put but with a delayed payoff. Drawing from the option pricing literature, it is widely acknowledged that the boundary for a finite-maturity American put gradually rises towards the strike, denoted as C/r in this context, as the time t approaches maturity T . The pricing problem for a finite-horizon American put is challenging due to the absence of analytical solutions, even for the simplest cases such as geometric Brownian motion. Consequently, numerical methods become essential for addressing this complexity.

We adopt the least-square Monte Carlo method (LSM), introduced by Longstaff and Schwartz (2001), due to its simplicity of implementation and reduced susceptibility to numerical stability issues. We conduct simulations with $N = 10^6$ sample paths, resulting in a numerical error of $O(1/10^3)$, which is adequate for our analysis. For our investigation, we consider three values for the terminal period T : 3, 6, and 10 years. We set 40 steps per year, denoted as $dt = 1/40$. Consequently, we allow for 40 exercise opportunities each year. Given that the examined horizon extends beyond one year, the simulated sample paths exhibit ample variations. Hence, the choice of 40 steps per year ensures the precision necessary for our analysis.

Table 8 displays the numerical results across Panels A to C, with additional quantities in Panel D for the infinite horizon case, extracted from Table 4, for ease of comparison. In the finite-maturity scenario, where the optimal boundary is no longer a constant, we focus solely on presenting the AD price of disinvestment and the project value. We perform the computations under ambiguity, employing our baseline configuration with $h_W/h = 0.5$ and utilizing 60 years of monthly data. As previously, results are provided for delay values $\delta \in \{0, 3\}$.

[Insert Table 8 about here]

The pivotal observation from Table 8 underscores the heightened joint impact of delay and ambiguity on disinvestment within a shorter horizon. Specifically, in scenarios lacking ambiguity, delay results in a 9.94% reduction in the AD price at $T = 3$. However, under ambiguity, this reduction intensifies to 24.72%. Similar patterns are evident at $T = 6$, where the reductions are 7.39% and 19.19%, respectively. As the horizon extends to 10 years, the AD prices gradually converge towards their infinite horizon benchmarks from above. The lower AD prices for short horizons, compared to the infinite horizon (0.470 versus 0.482; 0.370 versus 0.410), indi-

cates a tendency to postpone disinvestment. Thus, *Short Horizon* amplifies *Conservatism* when interacting with *Miscalibration* and *Sticky Policy*.

This outcome can be interpreted as an interplay among three categories of uncertainties. The first category of uncertainty stems from the stochastic nature of the state process, and its impact on the disinvestment boundary is delineated by the Uncertainty Multiplier in Equation (14). The second category pertains to payoff uncertainty induced by the delay, and its influence is encapsulated by the Delay Multiplier in Equation (14). The first-best disinvestment threshold under an infinite horizon is affected solely by these two forms of uncertainty.

However, under a finite horizon, the disinvestment threshold is additionally influenced by hitting time uncertainty. Clearly, hitting time uncertainty is more pronounced for a shorter horizon, so is payoff uncertainty. Therefore, as T increases, the role of payoff uncertainty diminishes, elucidating why delay is more salient for smaller values of T . Moreover, the worst-case scenario for the ambiguity-averse agent is characterized by the highest conceivable mean growth rate, and the delay effect increases with the mean growth rate.

These results offer additional novel testable implications concerning the interplay among planning horizon, ambiguity, and implementation delay. We hypothesize that when all three factors are at play, managers will assign lower valuations or higher discount rates to their projects.

3.5 Empirical implications

3.5.1 Testable implications

We summarize the testable implications derived from our results, with a particular focus on the determination of discount rates—a central issue in capital budgeting. While our findings directly pertain to project valuation, we can infer variations in discount rates across different scenarios, given that the cash flow structures are consistent. Specifically, we examine how the key components of our model—risk structure, ambiguity structure, and delay—impact the discount rate.

We hypothesize the following:

1. *Ambiguity and delay independently and jointly increase the discount rate.* Our results show that each factor alone lowers project value, with an additional reduction when both interact.

2. *For industries with the same objective volatility and jump parameters, differences in concerns over drift versus jump ambiguity lead to variations in discount rates.* Specifically, managers in industries where both types of ambiguity are significant tend to apply higher discount rates. This aligns with our finding that the disinvestment option value is lowest when both ambiguities are present.
3. *In industries without ambiguity, delay effects on the discount rate are independent of the objective variance structure. Under ambiguity, this is no longer true.* This is because the delay effect depends on the mean growth rate parameter, which ambiguity can distort.
4. *In industries without ambiguity, delay effects on the discount rate are independent of ex ante skewness. Under ambiguity, negative skewness in the return process amplifies the effect of delay.* This follows from the finding that the worst-case mean growth rate is highest when negative skewness exists under the reference measure.
5. *Short planning horizons increase discount rates and interact with both ambiguity and delay.* This is supported by our result that short horizons reduce the disinvestment option value, with stronger effects when both delay and ambiguity are present.

3.5.2 The five themes of Graham (2022)

Our results reveal intricate connections among the five themes, indicating that some themes can lead to others. For instance, one clear relationship is that *Miscalibration* can cause *Conservative Policy*. The challenges of calibrating risk structure, ambiguity structure, and determining the ambiguity level accentuate this tendency towards conservatism. Additionally, a *Short Horizon* can intensify conservativeness when interacting with *Miscalibration*. It is important to note that our model explicitly incorporates *Miscalibration* with jump ambiguity while treating the planning horizon as exogenous. Future research should explore generating *Short Horizon* as a consequence of the decision-making process.

In our model, *Sticky Policy* emerges as both a consequence and a potential amplification mechanism if considered a cause. Although we model *Sticky Policy* through implementation delay, we generate *Sticky Policy* as an outcome without relying on it as a cause. We predict that when ambiguity is sufficiently high, the agent will stick to immediate disinvestment regardless of delay. If *Sticky Policy* is interpreted as a result of inertia, in line with Graham (2022)

and others, it can interact with *Miscalibration* and *Short Horizon*, potentially intensifying policy conservativeness.

Lastly, *Simple Rule* is a consequence in our model. We show that elevated ambiguity can push the real option disinvestment threshold towards the NPV threshold. This implies that even if an agent chooses the optimal disinvestment threshold using real option analysis *ex ante*, ambiguity might cause the *ex post* threshold to approximate the NPV threshold, creating the perception of suboptimal decision-making. Moreover, *Short Horizon* can also contribute to this perception, as the optimal threshold under a short horizon is higher than under an infinite horizon due to hitting time uncertainty. Over time, under a short horizon, the optimal threshold will converge towards the NPV threshold, a phenomenon that does not depend on ambiguity.

3.5.3 The empirical literature

Our result under high ambiguity resolves the puzzling surge in disinvestment outlined by Winger and Rujana (2021) and Pagano and Zechner (2022). According to Proposition 2 and 4, elevated ambiguity fosters a strong demand for immediate divestiture. Importantly, this outcome is not a consequence of the volatility risk effect, which would typically postpone disinvestment. This is because volatility risk lowers the disinvestment boundary and amplifies the option value for divestiture rather than diminishing it.

Our result under moderate ambiguity offers a unified interpretation of recent empirical findings. Several of these studies highlight significant reductions in disinvestment attributed to heightened “uncertainty.” Notably, these empirical investigations do not differentiate between diffusion risk, jump risk, drift ambiguity, and jump ambiguity. Relevant studies include Jens (2017), Carvalho (2018), Campello et al. (2021), and Campello et al. (2022), among others.

Jens (2017) specifically highlights the amplified impact of economic policy uncertainty on the disinvestment activities of small firms and those in politically sensitive industries. Given that small firms and sensitive industries face higher levels of ambiguity, and the closer association of economic policy uncertainty with ambiguity rather than risk, our findings align with a more pronounced uncertainty effect on these firms. Notably, recent empirical studies, such as Aït-Sahalia et al. (2024), utilize the Economic Policy Uncertainty index introduced by Baker et al. (2016) as a measure for ambiguity.

Moreover, Humphery-Jenner et al. (2019) observe that disinvestment experience plays a pivotal role in shaping disinvestment decisions, particularly in optimizing timing. They emphasize

that optimal timing is key to maximize the return to shareholders. Since Epstein and Schneider (2007) offer the theoretical possibility that learning can reduce the perceived level of ambiguity, according to our model, a richer disinvestment experience is equivalent to a longer learning process, contributing to a reduced perceived level of ambiguity, thereby fostering more efficient disinvestment.

Additionally, Campello et al. (2021) demonstrate that secondary market liquidity for real assets can mitigate the uncertainty effect. In a similar vein, Campello et al. (2022) highlight that the reversibility of capital and labor can modulate the uncertainty effect. As in our model, one of the causes of implementation delay lies in the secondary market illiquidity for real assets. Consequently, a more prolonged implementation delay intensifies the impact of uncertainty.

4 Conclusion

This paper explores the complex interplay among five key themes in corporate decision-making—*Short Horizon*, *Miscalibration*, *Conservative Policy*, *Sticky Policy*, and *Simple Rule*—within the context of real options theory and disinvestment decisions. We develop a model that explicitly incorporates *Miscalibration*, accounting for both drift and jump ambiguity, and applies a double-exponential jump diffusion process to capture the full spectrum of upside and downside surprises. Our analysis reveals intricate connections among these themes, illustrating that *Miscalibration* often leads to *Conservative Policy* and that *Short Horizon* can exacerbate this conservatism.

We find that under high ambiguity, disinvestment is driven primarily by ambiguity aversion, leading agents to act immediately regardless of delay. This finding helps explain the surge in disinvestment observed during the COVID-19 pandemic. Under moderate ambiguity, our model provides new insights into empirical findings by showing how heightened uncertainty affects disinvestment decisions. Specifically, we demonstrate that increased ambiguity and implementation delay can raise discount rates and influence the disinvestment threshold, contributing to the perception of suboptimal decision-making.

Our results not only bridge the gap between real options literature on ambiguity and delay but also highlight how *Sticky Policy* and *Simple Rule* can arise as consequences of high ambiguity and its interplay with other themes. This comprehensive view advances our understanding of corporate disinvestment behavior and offers testable implications for future research.

References

- Aït-Sahalia, Y. and Jacod, J. (2012). Analyzing the Spectrum of Asset Returns: Jump and Volatility Components in High Frequency Data. *Journal of Economic Literature*, 50(4):1007–1050.
- Aït-Sahalia, Y. and Matthys, F. (2019). Robust consumption and portfolio policies when asset prices can jump. *Journal of Economic Theory*, 179:1–56.
- Aït-Sahalia, Y., Matthys, F., Osambela, E., and Sircar, R. (2024). When uncertainty and volatility are disconnected: Implications for asset pricing and portfolio performance. *Journal of Econometrics*, page 105654.
- Alvarez, L. H. R. and Keppo, J. (2002). The impact of delivery lags on irreversible investment under uncertainty. *European Journal of Operational Research*, 136(1):173–180.
- Alvarez, L. H. R. and Stenbacka, R. (2006). Takeover Timing, Implementation Uncertainty, and Embedded Divestment Options. *Review of Finance*, 10(3):417–441.
- Anderson, E. W., Hansen, L. P., and Sargent, T. J. (2003). A Quartet of Semigroups for Model Specification, Robustness, Prices of Risk, and Model Detection. *Journal of the European Economic Association*, 1(1):68–123.
- Attaoui, S., Cao, W., Duan, X., and Liu, H. (2021). Optimal capital structure, ambiguity aversion, and leverage puzzles. *Journal of Economic Dynamics and Control*, 129:104176.
- Baillon, A., Huang, Z., Selim, A., and Wakker, P. P. (2018). Measuring Ambiguity Attitudes for All (Natural) Events. *Econometrica*, 86(5):1839–1858.
- Baker, S. R., Bloom, N., and Davis, S. J. (2016). Measuring Economic Policy Uncertainty. *The Quarterly Journal of Economics*, 131(4):1593–1636.
- Bakshi, G., Cao, C., and Chen, Z. (1997). Empirical Performance of Alternative Option Pricing Models. *The Journal of Finance*, 52(5):2003–2049.
- Bar-Ilan, A. and Strange, W. C. (1996). Investment Lags. *The American Economic Review*, 86(3):610–622.

- Barry, J. W., Campello, M., Graham, J. R., and Ma, Y. (2022). Corporate flexibility in a time of crisis. *Journal of Financial Economics*, 144(3):780–806.
- Ben-David, I. and Chinco, A. M. (2023). Modeling managers as eps maximizers.
- Bolton, P., Chen, H., and Wang, N. (2011). A Unified Theory of Tobin's q, Corporate Investment, Financing, and Risk Management. *The Journal of Finance*, 66(5):1545–1578.
- Campello, M., Cortes, G. S., d'Almeida, F., and Kankanhalli, G. (2022). Exporting Uncertainty: The Impact of Brexit on Corporate America. *Journal of Financial and Quantitative Analysis*, 57(8):3178–3222.
- Campello, M., Kankanhalli, G., and Kim, H. (2021). Delayed creative destruction: How uncertainty shapes corporate assets. *NBER Working Paper No. 28971*.
- Cao, W., Duan, X., and Liu, H. (2022). Financing innovation under ambiguity. *Available at SSRN 4147887*.
- Carvalho, D. R. (2018). Uncertainty and exit decisions: Evidence from plant-level data. *Available at SSRN 2670926*.
- Chabi-Yo, F. (2012). Pricing kernels with stochastic skewness and volatility risk. *Management Science*, 58(3):624–640.
- Charoenwong, B., Kimura, Y., Kwan, A., and Tan, E. (2024). Capital budgeting, uncertainty, and misallocation. *Journal of Financial Economics*, 153:103779.
- Chen, N. and Kou, S. G. (2009). Credit Spreads, Optimal Capital Structure, and Implied Volatility with Endogenous Default and Jump Risk. *Mathematical Finance*, 19(3):343–378.
- Chen, Z. and Epstein, L. (2002). Ambiguity, Risk, and Asset Returns in Continuous Time. *Econometrica*, 70(4):1403–1443.
- Cheng, X. and Riedel, F. (2013). Optimal stopping under ambiguity in continuous time. *Mathematics and Financial Economics*, 7(1):29–68.
- Conrad, J., Dittmar, R. F., and Ghysels, E. (2013). Ex Ante Skewness and Expected Stock Returns. *The Journal of Finance*, 68(1):85–124.

- DeAngelo, H. (2022). The Capital Structure Puzzle: What Are We Missing? *Journal of Financial and Quantitative Analysis*, 57(2):413–454.
- Décamps, J.-P., Mariotti, T., Rochet, J.-C., and Villeneuve, S. (2011). Free cash flow, issuance costs, and stock prices. *The Journal of Finance*, 66(5):1501–1544.
- Delaney, L. (2021). A model of investment under uncertainty with time to build, market incompleteness and risk aversion. *European Journal of Operational Research*, 293(3):1155–1167.
- Delaney, L. (2022). The impact of operational delay on irreversible investment under Knightian uncertainty. *Economics Letters*, 215:110494.
- Dessaint, O., Foucault, T., and Frésard, L. (2023). The horizon of investors' information and corporate investment. *HEC Paris Research Paper No. FIN-2022-1462, Swiss Finance Institute Research Paper*, (23-03).
- Dixit, A. K. and Pindyck, R. S. (1994). *Investment under uncertainty*. Princeton university press.
- Drechsler, I. (2013). Uncertainty, Time-Varying Fear, and Asset Prices. *The Journal of Finance*, 68(5):1843–1889.
- Ellsberg, D. (1961). Risk, Ambiguity, and the Savage Axioms. *The Quarterly Journal of Economics*, 75(4):643–669.
- Epstein, L. G. and Schneider, M. (2007). Learning Under Ambiguity. *The Review of Economic Studies*, 74(4):1275–1303.
- Eraker, B., Johannes, M., and Polson, N. (2003). The Impact of Jumps in Volatility and Returns. *The Journal of Finance*, 58(3):1269–1300.
- Flor, C. R. and Hesel, S. (2015). Uncertain dynamics, correlation effects, and robust investment decisions. *Journal of Economic Dynamics and Control*, 51:278–298.
- Fukui, M., Gormsen, N. J., and Huber, K. (2024). Sticky discount rates. *Available at masao-fukui.github.io*.
- Geelen, T., Hajda, J., Morellec, E., and Winegar, A. (2024). Asset life, leverage, and debt maturity matching. *Journal of Financial Economics*, 154:103796.

- Gilboa, I. and Schmeidler, D. (1989). Maxmin expected utility with non-unique prior. *Journal of Mathematical Economics*, 18(2):141–153.
- Goldstein, R., Ju, N., and Leland, H. (2001). An EBIT-Based Model of Dynamic Capital Structure. *The Journal of Business*, 74(4):483–512.
- Graham, J. R. (2022). Presidential Address: Corporate Finance and Reality. *The Journal of Finance*, 77(4):1975–2049.
- Hannan, M. T. and Freeman, J. (1977). The population ecology of organizations. *American journal of sociology*, 82(5):929–964.
- Hannan, M. T. and Freeman, J. (1984). Structural inertia and organizational change. *American sociological review*, pages 149–164.
- Humphery-Jenner, M., Powell, R., and Zhang, E. J. (2019). Practice makes progress: Evidence from divestitures. *Journal of Banking & Finance*, 105:1–19.
- Jens, C. E. (2017). Political uncertainty and investment: Causal evidence from U.S. gubernatorial elections. *Journal of Financial Economics*, 124(3):563–579.
- Jeon, H. (2021). Investment and financing decisions in the presence of time-to-build. *European Journal of Operational Research*, 288(3):1068–1084.
- Kim, H. and Kung, H. (2017). The Asset Redeployability Channel: How Uncertainty Affects Corporate Investment. *The Review of Financial Studies*, 30(1):245–280.
- Kou, S. G. (2002). A Jump-Diffusion Model for Option Pricing. *Management Science*, 48(8):1086–1101.
- Kou, S. G. and Wang, H. (2003). First Passage Times of a Jump Diffusion Process. *Advances in Applied Probability*, 35(2):504–531.
- Kou, S. G. and Wang, H. (2004). Option Pricing Under a Double Exponential Jump Diffusion Model. *Management Science*, 50(9):1178–1192.
- Lambrecht, B. M. and Myers, S. C. (2007). A Theory of Takeovers and Disinvestment. *The Journal of Finance*, 62(2):809–845.

- Leland, H. E. (1998). Agency Costs, Risk Management, and Capital Structure. *The Journal of Finance*, 53(4):1213–1243.
- Li, S. and Wang, H. (2023). Robust irreversible investment strategy with ambiguity to jump and diffusion risk. *International Review of Finance*, 23(3):645–665.
- Longstaff, F. A. and Schwartz, E. S. (2001). Valuing American Options by Simulation: A Simple Least-Squares Approach. *The Review of Financial Studies*, 14(1):113–147.
- Maccheroni, F., Marinacci, M., and Rustichini, A. (2006). Dynamic variational preferences. *Journal of Economic Theory*, 128(1):4–44.
- Maenhout, P. J. (2006). Robust portfolio rules and detection-error probabilities for a mean-reverting risk premium. *Journal of Economic Theory*, 128(1):136–163.
- Merton, R. C. (1980). On estimating the expected return on the market: An exploratory investigation. *Journal of Financial Economics*, 8(4):323–361.
- Miao, J. and Rivera, A. (2016). Robust Contracts in Continuous Time. *Econometrica*, 84(4):1405–1440.
- Miao, J. and Wang, N. (2011). Risk, uncertainty, and option exercise. *Journal of Economic Dynamics and Control*, 35(4):442–461.
- Morellec, E., Nikolov, B., and Schürhoff, N. (2012). Corporate Governance and Capital Structure Dynamics. *The Journal of Finance*, 67(3):803–848.
- Nishimura, K. G. and Ozaki, H. (2004). Search and Knightian uncertainty. *Journal of Economic Theory*, 119(2):299–333.
- Nishimura, K. G. and Ozaki, H. (2007). Irreversible investment and Knightian uncertainty. *Journal of Economic Theory*, 136(1):668–694.
- Øksendal, B. and Sulem, A. (2019). *Applied Stochastic Control of Jump Diffusions*. Springer, Universitext.
- Pagano, M. and Zechner, J. (2022). COVID-19 and Corporate Finance. *The Review of Corporate Finance Studies*, 11(4):849–879.

- Quenez, M.-C. and Sulem, A. (2013). BSDEs with jumps, optimization and applications to dynamic risk measures. *Stochastic Processes and their Applications*, 123(8):3328–3357.
- Quenez, M.-C. and Sulem, A. (2014). Reflected BSDEs and robust optimal stopping for dynamic risk measures with jumps. *Stochastic Processes and their Applications*, 124(9):3031–3054.
- Ramey, V. A. and Shapiro, M. D. (2001). Displaced Capital: A Study of Aerospace Plant Closings. *Journal of Political Economy*, 109(5):958–992.
- Sandri, S., Schade, C., Mußhoff, O., and Odening, M. (2010). Holding on for too long? An experimental study on inertia in entrepreneurs' and non-entrepreneurs' disinvestment choices. *Journal of Economic Behavior & Organization*, 76(1):30–44.
- Sarkar, S. and Zhang, C. (2013). Implementation lag and the investment decision. *Economics Letters*, 119(2):136–140.
- Sarkar, S. and Zhang, C. (2015). Investment policy with time-to-build. *Journal of Banking & Finance*, 55:142–156.
- Seo, K. (2009). Ambiguity and Second-Order Belief. *Econometrica*, 77(5):1575–1605.
- Strebulaev, I. A. (2007). Do Tests of Capital Structure Theory Mean What They Say? *The Journal of Finance*, 62(4):1747–1787.
- Thijssen, J. J. J. (2010). Irreversible investment and discounting: An arbitrage pricing approach. *Annals of Finance*, 6(3):295–315.
- Thijssen, J. J. J. (2011). Incomplete markets, ambiguity, and irreversible investment. *Journal of Economic Dynamics and Control*, 35(6):909–921.
- Thijssen, J. J. J. (2015). A model for irreversible investment with construction and revenue uncertainty. *Journal of Economic Dynamics and Control*, 57:250–266.
- Thywissen, C., Pidun, U., and zu Knyphausen-Aufseß, D. (2017). Divesting on time: How decision-making processes influence divestiture outcomes. *Available at SSRN 2961827*.
- Tsyplakov, S. (2008). Investment frictions and leverage dynamics. *Journal of Financial Economics*, 89(3):423–443.

Winger, J. and Rujana, J. (2021). Divesting during covid-19. *Bain & Company*.

A Appendix: Proofs

Proof of Proposition 1

Proof. Denote

$$\begin{aligned} V(0, \tau + \delta) &= X(0) - \frac{C}{r} + \inf_{Q^\theta} V_1(0, \tau + \delta, \theta) \\ &= X(0) - \frac{C}{r} + \inf_{Q^\theta} \mathbb{E}_0^\theta \left[e^{-r(\tau + \delta)} \left(\frac{C}{r} - X(\tau + \delta) \right) \right] \quad \text{for any } \tau \in \mathcal{T}_{0, T}. \end{aligned}$$

Hence, under Q^θ , $(V_1(t, \tau + \delta, \theta), \Sigma_1(t, \theta), K_1(t, u, \theta))$ is the solution of the following BSDE

$$-dV_1(t, \tau + \delta, \theta) = -\Sigma_1(t, \theta) dW^\theta(t) - \int_{\mathbb{R}} K_1(t, u, \theta) \tilde{N}^\theta(dt, du), \quad \text{for } t \in [0, \tau + \delta],$$

and $V_1(\tau + \delta, \tau + \delta, \theta) = C/r - X(\tau + \delta)$.

Then, by Girsanov, we have under Q^0

$$\begin{aligned} -dV_1(t, \tau + \delta, \theta) &= \left(-\Sigma_1(t, \theta) \theta_W(t) - \int_{\mathbb{R}} K_1(t, u, \theta) \theta_N(t, u) \nu(du) \right) dt - \Sigma_1(t, \theta) dW(t) \\ &\quad - \int_{\mathbb{R}} K_1(t, u, \theta) \tilde{N}(dt, du), \quad t \in [0, \tau + \delta], \end{aligned} \tag{A.1}$$

and $V_1(\tau + \delta, \tau + \delta, \theta) = C/r - X(\tau + \delta)$.

Meanwhile, by Itô formula, denote $f^\theta(t, X(t)) = V_1(t, \tau + \delta, \theta)$, we have

$$\begin{aligned} dV_1(t, \tau + \delta, \theta) &= f_t^\theta dt + f_x^\theta (\mu^\theta X(t) dt + \sigma X(t) dW^\theta(t)) + \frac{1}{2} \sigma^2 X^2(t) f_{xx}^\theta dt \\ &\quad + \int_{\mathbb{R}} \left(f^\theta(t, X(t^-) + (e^u - 1)X(t^-)) - f^\theta(t, X(t^-)) - f_x^\theta(t, X(t^-))(e^u - 1)X(t^-) \right) \nu^\theta(du) dt \\ &\quad + \int_{\mathbb{R}} \left(f^\theta(t, X(t^-) + (e^u - 1)X(t^-)) - f^\theta(t, X(t^-)) \right) \tilde{N}^\theta(dt, du). \end{aligned}$$

Hence, we have

$$\Sigma_1(t, \theta) = \sigma X(t) f_x^\theta(t, X(t)), \quad K_1(t, u, \theta) = f^\theta(t, e^u X(t^-)) - f^\theta(t, X(t^-)).$$

Since $V_1(t, \tau + \delta, \theta) = f^\theta(t, X(t))$ decreases in the x argument for all $t \in [0, \tau + \delta]$, we have $\Sigma_1(t, \theta) < 0$ and $-\Sigma_1(t, \theta)\theta_W(t) \geq \Sigma_1(t, \theta)\kappa$ for $\theta_W(t) \in [-\kappa, \kappa]$. Next, consider the dt term involving the integral in (A.1):

$$I^\theta = - \int_{\mathbb{R}} K_1(t, u, \theta) \theta_N(t, u) \nu(du) = I_+^\theta + I_-^\theta,$$

where

$$I_+^\theta = - \int_{\mathbb{R}^+} K_1(t, u, \theta) \theta_N(t, u) \nu(du), \quad I_-^\theta = - \int_{\mathbb{R}^-} K_1(t, u, \theta) \theta_N(t, u) \nu(du).$$

Since $K_1(t, u, \theta) < (>) 0$ on \mathbb{R}^+ (\mathbb{R}^-) by the monotonicity of f^θ with x , we have $I_+^\theta \geq 0$ and $I_-^\theta \geq - \int_{\mathbb{R}^+} K_1(t, u, \theta) (1 - e^{M_2 u}) \nu(du)$ for all t .

Denote $\theta^*(t) = (\theta_W^*(t), \theta_N^*(t, u)) = (-\kappa, 1 - \mathbf{1}_{u \geq 0} - e^{M_2 u} \mathbf{1}_{u < 0})$. Given the above, the linear driver in (A.1) is the smallest under $\theta^*(t)$ for all $(V_1(t, \tau + \delta, \theta), \Sigma_1(t, \theta), K_1(t, u, \theta))$. Hence, by the comparison theorem for BSDE with jumps (Quenez and Sulem, 2013), $V_1(0, \tau + \delta, \theta^*)$ is the smallest. \square

Proof of Proposition 2

Proof. We prove the statement with contraction by supposing $\tau^* > 0$.

Proposition 1 indicates that under Q^{θ^*} , $X(t)$ follows

$$dX(t)/X(t^-) = \mu^* dt + \sigma dW^{\theta^*}(t) + \int_{\mathbb{R}} (e^u - 1) \tilde{N}^{\theta^*}(dt, du)$$

where

$$\mu^* = \mu + \kappa\sigma + \left(\frac{\lambda q}{(\eta_2 + 1)} - \frac{\lambda q \eta_2}{(\eta_2^* + 1) \eta_2^*} \right).$$

Recall $V^\infty(0, \tau, \theta^*)$ is given by

$$V^\infty(0, \tau^*, \theta^*) = X(0) - \frac{C}{r} + \sup_{\tau \geq 0} \mathbb{E}_0^{\theta^*} [e^{-r(\tau + \delta)} (\frac{C}{r} - X(\tau + \delta))].$$

Let $Y(t) = \ln X(t)$. It suffices to evaluate the following

$$\begin{aligned}\mathbb{E}_\tau^{\theta^*} \left[e^{-r\delta} \left(\frac{C}{r} - X(\tau + \delta) \right) \right] &= \mathbb{E}_\tau^{\theta^*} \left[e^{-r\delta} \left(\frac{C}{r} - X(\tau) e^{Y(\tau+\delta) - Y(\tau)} \right) \right] \\ &= e^{-r\delta} \left(\frac{C}{r} - X(\tau) \mathbb{E}_0^{\theta^*} \left[e^{Y(\delta)} \right] \right) = e^{-r\delta} \left(\frac{C}{r} - e^{\mu^* \delta} X(\tau) \right).\end{aligned}$$

Hence,

$$V^\infty(0, \tau^*, \theta^*) = X(0) - \frac{C}{r} + \sup_{\tau \geq 0} e^{-r\delta} \mathbb{E}_0^{\theta^*} \left[e^{-r\tau} \left(\frac{C}{r} - e^{\mu^* \delta} X(\tau) \right) \right]. \quad (\text{A.2})$$

For convenience, we denote $V_1(X(0)) = \mathbb{E}_0^{\theta^*} \left[e^{-r\tau^*} \left(\frac{C}{r} - e^{\mu^* \delta} X(\tau^*) \right) \right] = \mathbb{E}_0^{\theta^*} [g(\tau^*, X(\tau^*))]$. Following Øksendal and Sulem (2019), we introduce $X_1(t) = (s + t, X(t))$ with $X_1(0) = (s, x)$. Then the generator of $X_1(t)$ is

$$\mathcal{A}\phi(s, x) = \frac{\partial \phi}{\partial s} + \mu^* x \frac{\partial \phi}{\partial x} + \frac{1}{2} \sigma^2 x^2 \frac{\partial^2 \phi}{\partial x^2} + \int_{\mathbb{R}} \left(\phi(s, xe^u) - \phi(s, x) - x(e^u - 1) \frac{\partial \phi}{\partial x} \right) \nu^{\theta^*}(du).$$

Hence, $V_1(X(0))$ is a special case of $V_1(X_1(0)) = \mathbb{E}_0^{\theta^*} [g(X_1(\tau^*))]$ for $s = 0$.

By Dynkin's formula, we have

$$\mathbb{E}_0^{\theta^*} [g(\tau^*, X(\tau^*))] = g(s, x) + \mathbb{E}_0^{\theta^*} \left[\int_0^{\tau^*} \mathcal{A}g(X_1(t)) dt \right]. \quad (\text{A.3})$$

Since the payoff function $g(s, x) = e^{-rs} \left(\frac{C}{r} - ax \right)$ with $a = e^{\mu^* \delta} > 0$, we have

$$\begin{aligned}\mathcal{A}g(s, x) &= -re^{-rs} \left(\frac{C}{r} - ax \right) - \mu^* axe^{-rs} + \int_{\mathbb{R}} \left(e^{-rs} \left(\frac{C}{r} - axe^u \right) - e^{-rs} \left(\frac{C}{r} - ax \right) + x(e^u - 1)ae^{-rs} \right) \nu^{\theta^*}(du) \\ &= e^{-rs} (a(r - \mu^*)x - C).\end{aligned} \quad (\text{A.4})$$

Hence, (A.3) becomes

$$\mathbb{E}_0^{\theta^*} [g(\tau, X(\tau))] = g(s, x) + \mathbb{E}_0^{\theta^*} \left[\int_0^{\tau} e^{-r(s+t)} (a(r - \mu^*)X(t) - C) dt \right]. \quad (\text{A.5})$$

If $r - \mu^* \leq 0$, the integrand in (A.5) is strictly negative, since $X(t)$ can never be negative and $C > 0$. Hence, $g(s, x) > \mathbb{E}_0^{\theta^*} [g(\tau, X(\tau))]$, contradicting with $\tau^* > 0$.

Thus, we have proven if the inequality in the statement holds, $\tau^* = 0$.

Furthermore, define

$$U = \{(s, x) \in \mathbb{R}^2; \mathcal{A}g(s, x) > 0\}.$$

Then (A.4) indicates that

$$U = \left\{ \mathbb{R} \times \left(-\infty, \frac{C}{a(r - \mu^*)} \right) \right\}, \quad \text{for } r < \mu^*.$$

Hence, according to (A.3) or (A.5), we have

$$\mathbb{E}_0^{\theta^*} [g(\tau^*, X(\tau^*))] < g(s, x) \quad \text{if } x \notin U \quad \text{and} \quad \tau^* > 0.$$

Proposition 3.3 of Øksendal and Sulem (2019) indicates that the continuation region D is a subset of U , i.e., $D \subset U$. Thus, we have shown that the continuation region D for $r < \mu^*$ is of the form

$$D = (-\infty, x^*), \quad \text{with} \quad x^* < \frac{C}{a(r - \mu^*)}.$$

Lastly, for $r = \mu^*$, (A.5) indicates that $\mathbb{E}_0^{\theta^*} [g(\tau, X(\tau))] < g(s, x)$ for any $x \in \mathbb{R}$ if $\tau^* > 0$. Hence, $D = \emptyset$.

□

Proof of Proposition 3

Proof. In the proof of Proposition 2, Equation (A.2) indicates that we can evaluate the following

$$V_1^\infty(0, \tau^*, \theta^*) = \sup_{\tau > 0} e^{-r\delta} \mathbb{E}_0^{\theta^*} \left[e^{-r\tau} \left(\frac{C}{r} - e^{\mu^*\delta} X(\tau) \right) \right].$$

Note that in the above, we are looking for $\tau^* > 0$, because the reverse of inequality (11) ensures that.

The functional form inside the conditional expectation entails that the optimal stopping time is of the threshold type $\tau^* = \inf_t \{X(t) \leq X^*\}$. However, due to the “overshooting” problem caused by jumps, it is also possible that $X(\tau^*) < X^*$. Hence, we utilize the results from Kou and

Wang (2003) for the following

$$\mathbb{E}_0^{\theta^*} [e^{-r\tau}] = d_{1,0} \left(\frac{X_D}{x} \right)^{\beta_3} + d_{2,0} \left(\frac{X_D}{x} \right)^{\beta_4},$$

and

$$\mathbb{E}_0^{\theta^*} [e^{-r\tau} X(\tau)] = X_D \left[d_{1,1} \left(\frac{X_D}{x} \right)^{\beta_3} + d_{2,1} \left(\frac{X_D}{x} \right)^{\beta_4} \right],$$

where $\tau = \inf_t \{X(t) \leq X_D\}$ for some $X_D < X(0) = x$ and β_i and $d_{i,j}$ are given by (15) and (16).

Hence,

$$e^{r\delta} V_1^\infty(0, \tau^*, \theta^*) = \frac{C}{r} \left[d_{1,0} \left(\frac{X_D}{x} \right)^{\beta_3} + d_{2,0} \left(\frac{X_D}{x} \right)^{\beta_4} \right] - e^{\mu^* \delta} X_D \left[d_{1,1} \left(\frac{X_D}{x} \right)^{\beta_3} + d_{2,1} \left(\frac{X_D}{x} \right)^{\beta_4} \right].$$

Therefore, we can utilize the “smooth pasting” principle, or Theorem 3.2 of Øksendal and Sulem (2019), that $V_1^\infty(0, \tau^*, \theta^*)$ as a function of $X(0) = x$ should be C^1 at X^* to be optimal to find the free boundary X^* . Since for $x > X^*$,

$$e^{r\delta} \frac{\partial V_1^\infty}{\partial x} = A_1 X_D^{\beta_3} x^{-\beta_3-1} + A_2 X_D^{\beta_4} x^{-\beta_4-1} - A_3 X_D^{1+\beta_3} x^{-\beta_3-1} - A_4 X_D^{1+\beta_4} x^{-\beta_4-1},$$

with

$$A_1 = -\beta_3 d_{1,0} \frac{C}{r}, \quad A_2 = -\beta_4 d_{2,0} \frac{C}{r}, \quad A_3 = -\beta_3 d_{1,1} e^{\mu^* \delta}, \quad \text{and} \quad A_4 = -\beta_4 d_{2,1} e^{\mu^* \delta},$$

we have

$$e^{r\delta} \frac{\partial V_1^\infty}{\partial x} \Big|_{x \downarrow X^*} = A_1 / X^* + A_2 / X^* - A_3 - A_4.$$

Meanwhile for $x \leq X^*$,

$$e^{r\delta} \frac{\partial V_1^\infty}{\partial x} \Big|_{x \uparrow X^*} = -e^{\mu^* \delta}.$$

Hence,

$$X^* = e^{-\mu^* \delta} \frac{\beta_3 \beta_4 (\eta_2^* + 1)}{(\beta_3 + 1)(\beta_4 + 1) \eta_2^*} \frac{C}{r}.$$

□

B Tables and figures

Table 2: **Characteristics of the Lévy measure under multiple priors.**

This table presents the characteristics of the Lévy measure under the reference measure Q^0 , alternative equivalent priors Q^θ for $\theta_{N,1}(t) \in [-M_1, 0]$ and $\theta_{N,2}(t) \in [0, M_2]$ and the worst-case measure Q^{θ^*} .

Quantity	Q^0	Q^θ	Q^{θ^*}
Jump intensity	λ	$\lambda_t^\theta \in \left[\lambda \left(\frac{p\eta_1}{\eta_1+M_1} + \frac{q\eta_2}{\eta_2+M_2} \right), \lambda \right]$	$\lambda^* = \lambda \left(p + \frac{q\eta_2}{\eta_2+M_2} \right)$
Cond. Prob. (positive jumps)	p	$p_t^\theta \in \left[\frac{p\eta_1}{p\eta_1+q(\eta_1+M_1)}, \frac{p(\eta_2+M_2)}{p(\eta_2+M_2)+q\eta_2} \right]$	$p^* = \frac{p(\eta_2+M_2)}{p(\eta_2+M_2)+q\eta_2}$
Cond. Prob. (negative jumps)	$q = 1 - p$	$q_t^\theta \in \left[\frac{q\eta_2}{p(\eta_2+M_2)+q\eta_2}, \frac{q(\eta_1+M_1)}{p\eta_1+q(\eta_1+M_1)} \right]$	$q^* = \frac{q\eta_2}{p(\eta_2+M_2)+q\eta_2}$
Cond. mean jump size (positive)	$\frac{1}{\eta_1}$	$\int_{\mathbb{R}^+} u f_t^\theta(du) \in \left[\frac{1}{\eta_1+M_1}, \frac{1}{\eta_1} \right]$	$\frac{1}{\eta_1}$
Cond. mean jump size (negative)	$\frac{-1}{\eta_2}$	$\int_{\mathbb{R}^-} u f_t^\theta(du) \in \left[\frac{-1}{\eta_2}, \frac{-1}{\eta_2+M_2} \right]$	$-\frac{1}{\eta_2+M_2}$

Table 3: **Benchmark parameter values.**

This table shows the benchmark parameter values for our numerical analyses and the central moments of $Y(t) = \ln(X(t))$ under these values for $t = 1$ under the reference measure Q^0 . r is the risk free rate. C is the maintenance cost. x is the initial asset value. The other process parameters can refer to Section.

A. Parameter values			
	Common value		
r	0.05		
C	1		
x	20		
μ	0.02		
σ	0.2		
λ	1		
p	0.5		
	$Skew^-$	$Skew^0$	$Skew^+$
η_1	7	7	4
η_2	4	7	7
B. Central moments of $Y(t) = \ln(X(t))$ for $t = 1$ under Q^0			
Moment	$Skew^-$	$Skew^0$	$Skew^+$
Mean	-0.037	-0.021	-0.051
Variance	0.123	0.081	0.123
Skewness	-0.885	0.000	0.885
Kurtosis	6.434	4.530	6.434

Table 4: **Disinvestment under ambiguity and implementation delay: Baseline.**

In Panel A, we report the detection-error probability calibration result. We report the relevant parameters and moment statistics (under $t = 1$) for $Y(t) = \ln(X(t))$ under the worst-case probability measure Q^{θ^*} at the maximum level of ambiguity h^* , such that the detection-error probability $\pi(n; h^*) = 0.1$. Q^{θ^*} - Quarter (Month) indicates the calibration sample consists of 60 years of quarterly (monthly) data, i.e., $n = 60 \times 4(12)$. In Panel B, we report the optimal disinvestment boundary X^* , the AD price of disinvestment $AD^* = \mathbb{E}_0^\theta[e^{-r\tau^*}]$ for $\theta \in \{0, \theta^*\}$, and the project value V^* under delay (δ). We set $h_W/h = 0.5$, i.e., the agent places equal concern for drift ambiguity versus jump ambiguity. The columns “(%) Change” reports the percentage change in the row quantity from $\delta = 0$ to $\delta = 3$. For example, $-5.82\% = (9.147 - 9.712) / 9.712 \times 100$ (%) for X^* under Q^0 .

Panel A: Detection-error probability calibration			
	Q^{θ^*} -Quarter	Q^{θ^*} -Month	
$h^* \times 10^4$	160.746	54.706	
$\kappa^* \times 10^2$	12.679	7.396	
M_2^*	1.016	0.559	
η_2^*	8.016	7.559	
λ^*	0.937	0.963	
p^*	0.534	0.519	
μ^*	0.059	0.043	
Mean	0.021	0.004	
Variance	0.074	0.077	
Skewness	0.182	0.109	
Kurtosis	4.376	4.431	
Panel B: Disinvestment under ambiguity and delay			
	$\delta = 0$	$\delta = 3$	(%) Change
Q^0			
X^*	9.712	9.147	-5.82
AD^*	0.508	0.482	-5.15
V^*	5.405	4.412	-18.36
Q^{θ^*} -Month			
X^*	11.236	9.871	-12.15
AD^*	0.478	0.410	-14.39
V^*	4.353	3.208	-26.30

Table 5: **Disinvestment under ambiguity and implementation delay: Ambiguity structure.**

In Panel A, we report the detection-error probability calibration results for drift ambiguity share $h_W/h \in \{0, 0.5, 1\}$. In Panel B, we report the optimal disinvestment boundary X^* , the AD price of disinvestment $AD^* = \mathbb{E}_0^{\theta^*} [e^{-rt^*}]$, and the project value V^* under delay (δ) at the maximum level of ambiguity h^* , such that the detection error probability $\pi(n; h^*) = 0.1$. $Q^{\theta^*} - Month$ indicates the calibration sample consists of 60 years of monthly data, i.e., $n = 60 \times 12$. The columns “(%) Change” reports the percentage change in the row quantity from $\delta = 0$ to $\delta = 3$.

Panel A: Detection-error probability calibration results			
	$h_W/h = 0$	$h_W/h = 0.5$	$h_W/h = 1$
$h^* \times 10^4$	43.484	54.706	65.838
$\kappa^* \times 10^2$	0.000	7.396	11.475
M_2^*	0.720	0.559	0.000
η_2^*	7.720	7.559	7.000
λ^*	0.953	0.963	1.000
p^*	0.524	0.519	0.500
μ^*	0.031	0.043	0.043
Mean	-0.008	0.004	0.002
Variance	0.076	0.077	0.081
Skewness	0.136	0.109	0.000
Kurtosis	4.410	4.431	4.530

Panel B: Disinvestment under ambiguity and delay			
	$\delta = 0$	$\delta = 3$	(%) Change
(a) $Q^{\theta^*} - Month h_W/h = 0$			
X^*	10.526	9.605	-8.75
AD^*	0.492	0.447	-9.16
V^*	4.799	3.752	-21.81
(b) $Q^{\theta^*} - Month h_W/h = 0.5$			
X^*	11.236	9.871	-12.15
AD^*	0.478	0.410	-14.39
V^*	4.353	3.208	-26.30
(c) $Q^{\theta^*} - Month h_W/h = 1$			
X^*	11.033	9.699	-12.09
AD^*	0.482	0.417	-13.58
V^*	4.525	3.366	-25.60

Table 6: Disinvestment under ambiguity and implementation delay: Variance structure and ambiguity structure.

In Panel A, we report the detection-error probability calibration results conditional on diffusion volatility σ and drift ambiguity share h_W/h . In Panel B, we report the optimal disinvestment boundary X^* , the AD price of disinvestment $AD^* = \mathbb{E}_0^{\theta^*} [e^{-r\tau^*}]$, and the project value V^* under delay (δ) at the maximum level of ambiguity h^* , such that the detection error probability $\pi(n; h^*) = 0.1$. The calibration sample consists of 60 years of monthly data, i.e., $n = 60 \times 12$. The columns “(%) Change” reports the percentage change in the row quantity from $\delta = 0$ to $\delta = 3$.

Panel A: Variance matching results						
	$\sigma = 0.15$			$\sigma = 0.25$		
$\eta_1 = \eta_2$	5.856			10.450		
Mean	-0.021			-0.020		
Variance	0.081			0.081		
Skewness	0.000			0.000		
Kurtosis	6.124			3.308		

Panel B: Detection-error probability calibration results						
	$\sigma = 0.15$			$\sigma = 0.25$		
	$h_W/h = 0$	$h_W/h = 0.5$	$h_W/h = 1$	$h_W/h = 0$	$h_W/h = 0.5$	$h_W/h = 1$
$h^* \times 10^4$	43.484	54.706	65.838	43.484	54.706	65.838
$\kappa^* \times 10^2$	0.000	7.396	11.475	0.000	7.396	11.475
M_2^*	0.602	0.468	0.000	1.075	0.835	0.000
η_2^*	6.459	6.324	5.856	11.524	11.284	10.450
λ^*	0.953	0.963	1.000	0.953	0.963	1.000
p^*	0.524	0.519	0.500	0.524	0.519	0.500
μ^*	0.032	0.041	0.037	0.027	0.044	0.049
Mean	-0.006	0.002	-0.004	-0.012	0.005	0.008
Variance	0.073	0.075	0.081	0.078	0.079	0.081
Skewness	0.243	0.193	0.000	0.039	0.031	0.000
Kurtosis	6.055	6.064	6.124	3.264	3.272	3.308

(Table 6 to be continued next page.)

(Table 6 continued.)

	$\sigma = 0.15$			$\sigma = 0.25$		
	$\delta = 0$	$\delta = 3$	(%) Change	$\delta = 0$	$\delta = 3$	(%) Change
	Q^0			Q^0		
X^*	9.980	9.399	-5.824	9.496	8.943	-5.824
AD^*	0.505	0.479	-5.114	0.511	0.485	-5.182
V^*	5.388	4.401	-18.328	5.418	4.421	-18.389
	$Q^{\theta^*} h_W/h = 0$			$Q^{\theta^*} h_W/h = 0$		
X^*	11.008	9.996	-9.192	10.009	9.217	-7.911
AD^*	0.483	0.435	-9.975	0.501	0.461	-7.813
V^*	4.629	3.587	-22.505	5.038	3.998	-20.654
	$Q^{\theta^*} h_W/h = 0.5$			$Q^{\theta^*} h_W/h = 0.5$		
X^*	11.488	10.165	-11.521	10.952	9.584	-12.489
AD^*	0.474	0.410	-13.469	0.483	0.412	-14.667
V^*	4.350	3.240	-25.504	4.414	3.242	-26.553
	$Q^{\theta^*} h_W/h = 1$			$Q^{\theta^*} h_W/h = 1$		
X^*	11.009	9.846	-10.563	11.096	9.588	-13.590
AD^*	0.484	0.430	-11.088	0.481	0.402	-16.279
V^*	4.718	3.611	-23.462	4.337	3.125	-27.939

Table 7: **Disinvestment under ambiguity and implementation delay: *Ex ante* skewness.**

In Panel A, we report the detection-error probability calibration results for $Skew^-$ and $Skew^+$ as in Table 3. In Panel B, we report the optimal disinvestment boundary X^* , the AD price of disinvestment $AD^* = \mathbb{E}_0^{\theta^*} [e^{-r\tau^*}]$, and the project value V^* under delay (δ) at the maximum level of ambiguity h^* , such that the detection error probability $\pi(n; h^*) = 0.1$. The calibration sample consists of 60 years of monthly data, i.e., $n = 60 \times 12$. We set $h_W/h = 0.5$. The columns “(%) Change” reports the percentage change in the row quantity from $\delta = 0$ to $\delta = 3$.

Panel A: Detection-error probability calibration results						
	$Skew^-$			$Skew^+$		
$h^* \times 10^4$	54.706			54.706		
$\kappa^* \times 10^2$	7.396			7.396		
M_2^*	0.319			0.559		
η_2^*	4.319			7.559		
λ^*	0.963			0.963		
p^*	0.519			0.519		
μ^*	0.048			0.043		
Mean	-0.004			-0.026		
Variance	0.110			0.119		
Skewness	-0.705			0.989		
Kurtosis	6.049			6.568		
Panel B: Disinvestment under ambiguity and delay						
	$Skew^-$			$Skew^+$		
	$\delta = 0$	$\delta = 3$	(%) Change	$\delta = 0$	$\delta = 3$	(%) Change
$X^* Q^0$	8.661	8.157	-5.82	7.627	7.183	-5.82
$AD^* Q^0$	0.536	0.516	-3.73	0.555	0.536	-3.47
$V^* Q^0$	6.564	5.439	-17.14	6.993	5.810	-16.92
$X^* Q^{\theta^*}$	10.319	8.942	-13.35	8.761	7.696	-12.15
$AD^* Q^{\theta^*}$	0.497	0.438	-11.84	0.528	0.479	-9.23
$V^* Q^{\theta^*}$	5.291	4.016	-24.09	6.045	4.723	-21.87

Table 8: Disinvestment under ambiguity and implementation delay: Finite horizon.

This table reports the AD price of disinvestment $AD^* = \mathbb{E}_0^\theta[e^{-r\tau^*}]$ for $\theta \in \{0, \theta^*\}$ and the project value V^* when the disinvestment horizon T is finite under delay. $Q^{\theta^*} - Month$ is calibrated with 60 years of monthly data. We set $h_W/h = 0.5$. The columns “(%) Change” reports the percentage change in the row quantity from $\delta = 0$ to $\delta = 3$. In Panels A to C, we report the quantities for $T = 3, 6, 10$ years, and we report the infinite horizon results from Table 4 in Panel D for reference.

	$\delta = 0$	$\delta = 3$	(%) Change	$\delta = 0$	$\delta = 3$	(%) Change
A. $T = 3$	Q^0			$Q^{\theta^*} - Month$		
AD^*	0.522	0.470	-9.94	0.492	0.370	-24.72
V^*	3.097	2.304	-25.63	2.678	1.593	-40.50
B. $T = 6$	Q^0			$Q^{\theta^*} - Month$		
AD^*	0.518	0.480	-7.39	0.485	0.392	-19.19
V^*	3.940	3.063	-22.27	3.314	2.193	-33.81
C. $T = 10$	Q^0			$Q^{\theta^*} - Month$		
AD^*	0.511	0.481	-6.03	0.478	0.399	-16.63
V^*	4.515	3.591	-20.46	3.729	2.594	-30.45
D. $T = +\infty$	Q^0			$Q^{\theta^*} - Month$		
AD^*	0.508	0.482	-5.15	0.478	0.410	-14.39
V^*	5.405	4.412	-18.36	4.353	3.208	-26.30

Figure 2: **Detection-error probability calibrations.** This figure plots calibration results for detection-error probability $\pi(n; h)$ where total ambiguity $h \in [0, h^*]$ with h^* satisfying $\pi(n; h^*) = 0.1$. The red solid (blue dashed) lines are based on $n = 60 \times 4$ quarterly ($n = 60 \times 12$ monthly) samples of $X(t)$. We set $h_W/h = 0.5$, i.e., the agent places equal concerns for drift ambiguity versus jump ambiguity.

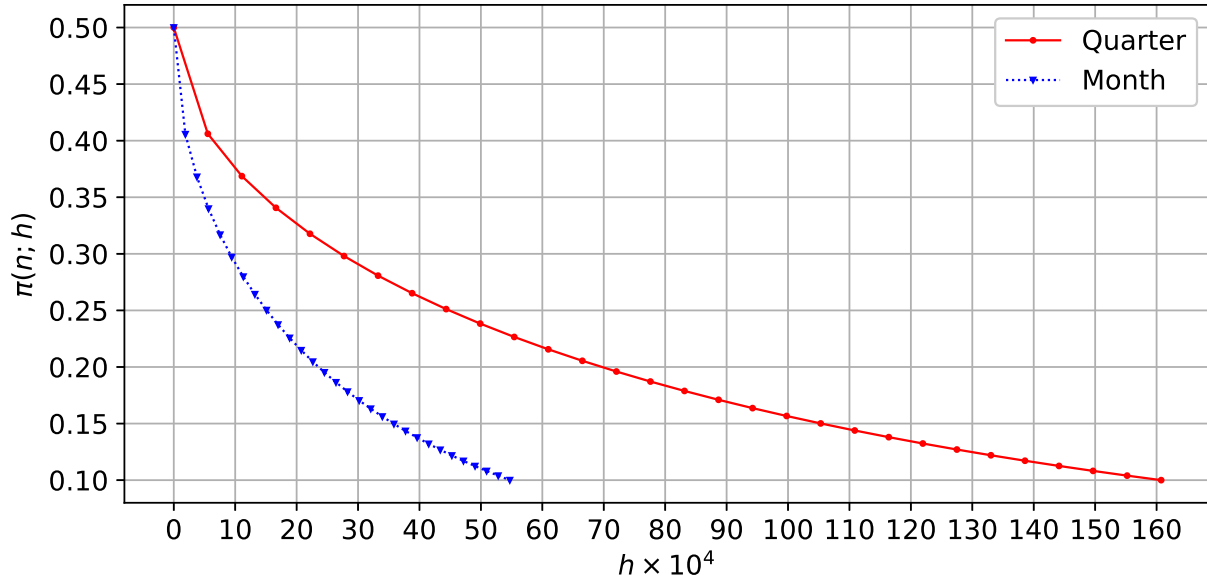
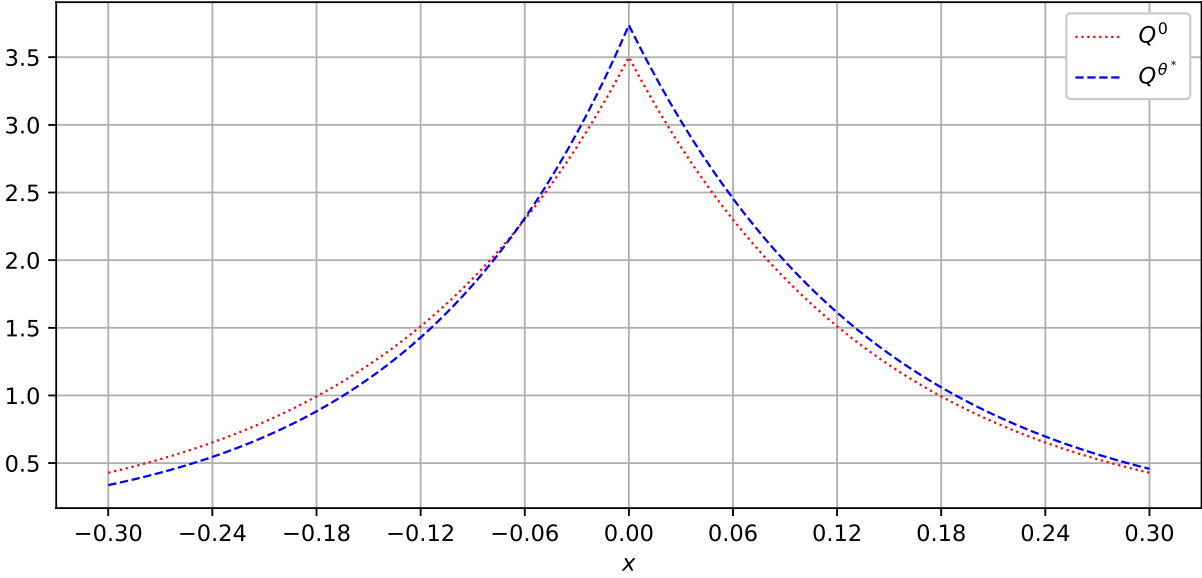
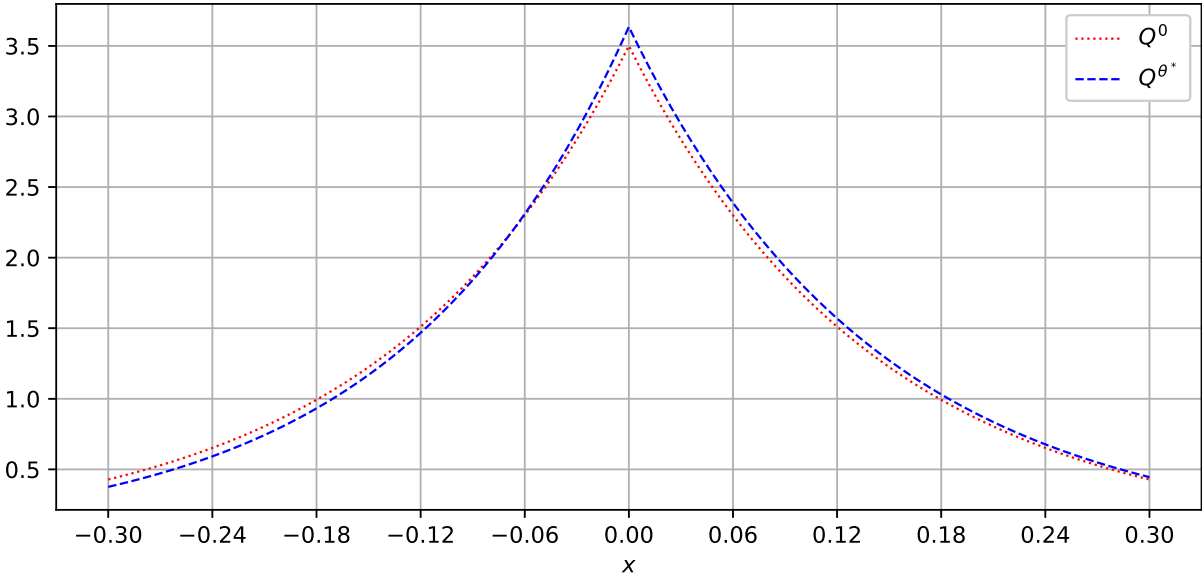


Figure 3: Jump size distributions. This figure plots the probability density function for the jump size of $Y(t)$ under the reference measure Q^0 and under the worst-case measure Q^{θ^*} where total ambiguity is set at $h = h^*$, such that $\pi(n; h^*) = 0.1$. The calibration of h^* uses $n = 60 \times 4$ quarterly ($n = 60 \times 12$ monthly) samples of $X(t)$. We set $h_W/h = 0.5$, i.e., the agent places equal concern for drift ambiguity versus jump ambiguity.

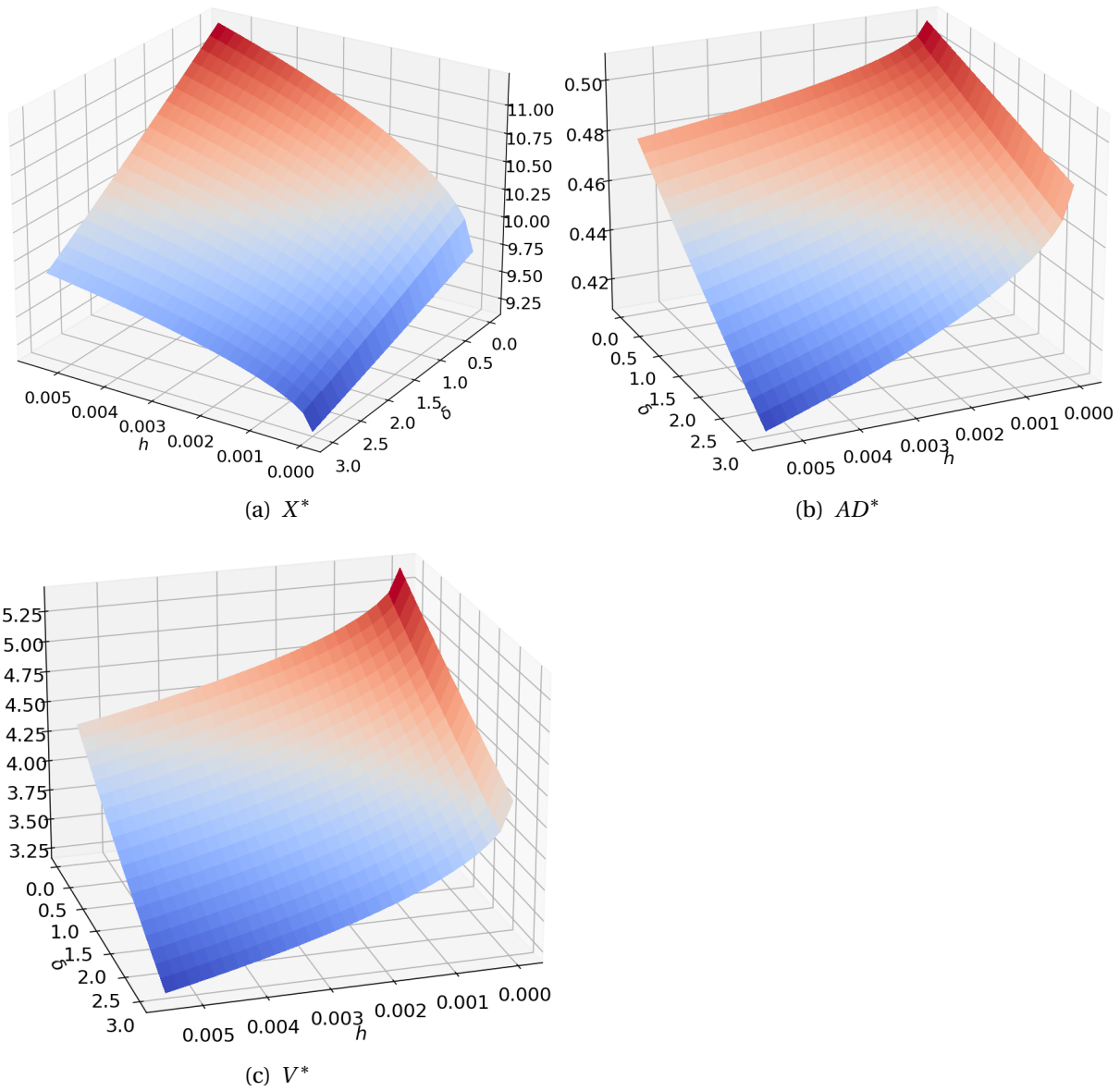


(a) Quarter



(b) Month
60

Figure 4: **Disinvestment under ambiguity and payoff delay: Baseline** This figure plots the optimal disinvestment boundary X^* , the AD price of disinvestment $AD^* = \mathbb{E}_0^{\theta^*} [e^{-r\tau^*}]$, and the project value V^* against total ambiguity level h and implementation delay δ . Q^{θ^*} is calibrated with 60 years of monthly data ($n = 60 \times 12$). We set $h_W/h = 0.5$, i.e., the agent places equal concern for drift ambiguity versus jump ambiguity. The h axis has a range $[0, h^*]$ with h^* satisfying $\pi(n; h^*) = 0.1$.



C Internet Appendix—Disinvestment under Ambiguity and Delay

This appendix provides additional technical results that support the main analysis in the draft.

C.1 The minimax property for the delayed optimal stopping problem

We summarize the key properties of the general optimal stopping under ambiguity problem studied by Quenez and Sulem (2013, 2014). Let g_t satisfy $\mathbb{E}[\sup_{0 \leq t \leq T} |g_t|^2] < +\infty$. Quenez and Sulem (2013) show that for $\theta = (\theta_W, \theta_N)$ given in Section 2.2, the (nonlinear) expectation $\inf_{Q^\theta} \mathbb{E}_S^\theta[g_\tau]$ is dynamically consistent for all $\theta \in \Theta$ and stopping times S, τ . We say $\inf_{Q^\theta} \mathbb{E}_S^\theta[g_\tau]$ is dynamically consistent if the following holds

$$\inf_{Q^\theta} \mathbb{E}_S^\theta[g_\tau] = \inf_{Q^{\theta'}} \mathbb{E}_S^{\theta'} \left[\inf_{Q^{\theta''}} \mathbb{E}_{S_1}^{\theta''}[g_\tau] \right], \quad \theta, \theta', \theta'' \in \Theta, \quad S_1 \in [S, \tau].$$

Dynamic consistency provides analytical convenience in that the worst-case density generator for $[S, \tau]$ coincides with the ones for $[S, S_1]$ and $[S_1, \tau]$ piece-wisely, and our main analysis relies on this property to evaluate conditional expectations. Moreover, Quenez and Sulem (2014) show that under the above conditions, the following holds

$$\sup_{\tau} \inf_{Q^\theta} \mathbb{E}^\theta[g_\tau] = \inf_{Q^\theta} \sup_{\tau} \mathbb{E}^\theta[g_\tau]. \quad (\text{C.1})$$

However, this property cannot be directly applied in our case, because our problem is a delayed optimal stopping problem. Nevertheless, we can utilize this property to prove that the minimax relation also holds under delay.

Lemma 1. *Let function g satisfy $\mathbb{E}_0[\sup_{0 \leq t \leq T} |g(X(t))|^2] < +\infty$ and $\delta > 0$ be independent of $X(t)$. Then,*

$$\sup_{\tau \in \mathcal{T}_{0,T}} \inf_{Q^\theta} \mathbb{E}_0^\theta[g(X(\tau + \delta))] = \inf_{Q^\theta} \sup_{\tau \in \mathcal{T}_{0,T}} \mathbb{E}_0^\theta[g(X(\tau + \delta))]. \quad (\text{C.2})$$

Proof. The idea is to transform the delayed optimal stopping problem under jump ambiguity to the one without delay so that we can apply the minimax relation—Equation (C.1).

Let $V_1 = \sup_{\tau \in \mathcal{T}_{0,T}} \inf_{Q^\theta} \mathbb{E}_0^\theta [g(X(\tau + \delta))]$. By dynamic consistency, we have

$$V_1 = \sup_{\tau \in \mathcal{T}_{0,T}} \inf_{Q^\theta} \mathbb{E}_0^\theta [g(X(\tau + \delta))] = \sup_{\tau \in \mathcal{T}_{0,T}} \inf_{Q^\theta} \mathbb{E}_0^\theta \left[\inf_{Q^\theta} \mathbb{E}_\tau^\theta [g(X(\tau + \delta))] \right].$$

Define $\hat{g}(X(\tau)) = \inf_{Q^\theta} \mathbb{E}_0^\theta [g(X(\delta)) | X(0) = X(\tau)]$. By the strong Markov property of $X(t)$ and the independence of δ , we can write V_1 as

$$V_1 = \sup_{\tau \in \mathcal{T}_{0,T}} \inf_{Q^\theta} \mathbb{E}_0^\theta [\hat{g}(X(\tau))].$$

Let $V_2 = \inf_{Q^\theta} \sup_{\tau \in \mathcal{T}_{0,T}} \mathbb{E}_0^\theta [g(X(\tau + \delta))]$. Then, we have

$$V_2 = \inf_{Q^\theta} \sup_{\tau \in \mathcal{T}_{0,T}} \mathbb{E}_0^\theta [g(X(\tau + \delta))] = \inf_{Q^\theta} \sup_{\tau \in \mathcal{T}_{0,T}} \mathbb{E}_0^\theta \left[\mathbb{E}_\tau^\theta [g(X(\tau + \delta))] \right].$$

Define $\bar{g}(X(\tau)) = \mathbb{E}_0^\theta [g(X(\delta)) | X(0) = X(\tau)]$. Then, we have

$$V_2 = \inf_{Q^\theta} \sup_{\tau \in \mathcal{T}_{0,T}} \mathbb{E}_0^\theta [\bar{g}(X(\tau))].$$

The above is a standard non-delayed stopping problem under jump ambiguity. So, we can apply Equation (C.1) to have

$$V_2 = \sup_{\tau \in \mathcal{T}_{0,T}} \inf_{Q^\theta} \mathbb{E}_0^\theta [\bar{g}(X(\tau))].$$

Again, by dynamic consistency, we have

$$V_2 = \sup_{\tau \in \mathcal{T}_{0,T}} \inf_{Q^\theta} \mathbb{E}_0^\theta [\bar{g}(X(\tau))] = \sup_{\tau \in \mathcal{T}_{0,T}} \inf_{Q^\theta} \mathbb{E}_0^\theta \left[\inf_{Q^\theta} \mathbb{E}_\tau^\theta [\bar{g}(X(\tau))] \right] = V_1.$$

□

C.2 Relative entropy growth

The key to this is the log of the Radon-Nikodym derivative $\zeta^{\theta^*}(t) = \ln(Z^{\theta^*}(t))$, where $Z^{\theta^*}(t) = dQ^{\theta^*} / dQ^0$. Under Q^0 , $Z^{\theta^*}(t)$ is

$$dZ^{\theta^*}(t) / Z^{\theta^*}(t^-) = -\theta_W(t) dW(t) - \int_{\mathbb{R}} \theta_N(t) \tilde{N}(dt, du).$$

Using the results for $\theta^*(t)$, we can write

$$dZ^{\theta^*}(t)/Z^{\theta^*}(t^-) = \kappa dW(t) - \int_{\mathbb{R}^-} (1 - e^{M_2 u}) \tilde{N}(dt, du).$$

Hence, by Itô formula, we have

$$\begin{aligned} Z^{\theta^*}(t) &= \exp\left(\kappa W(t) - \frac{1}{2}\kappa^2 t + \int_0^t \int_{\mathbb{R}^-} \ln(1 - (1 - e^{M_2 u})) \tilde{N}(ds, du)\right) \\ &\quad + \int_0^t \int_{\mathbb{R}^-} [\ln(1 - (1 - e^{M_2 u})) + 1 - e^{M_2 u}] \nu(du) ds \\ &= \exp\left(\kappa W(t) - \frac{1}{2}\kappa^2 t + \int_0^t \int_{\mathbb{R}^-} M_2 u \tilde{N}(ds, du) + \int_0^t \int_{\mathbb{R}^-} [M_2 u + 1 - e^{M_2 u}] \nu(du) ds\right) \\ &= \exp\left(\kappa W(t) - \frac{1}{2}\kappa^2 t + \int_0^t \int_{\mathbb{R}^-} M_2 u \tilde{N}(ds, du) + t \int_{\mathbb{R}^-} [M_2 u + 1 - e^{M_2 u}] \lambda q \eta_2 e^{\eta_2 u} du\right) \\ &= \exp\left(\kappa W(t) - \frac{1}{2}\kappa^2 t + \int_0^t \int_{\mathbb{R}^-} M_2 u \tilde{N}(ds, du) - t \lambda q \eta_2 \left[\frac{M_2}{\eta_2^2} - \frac{1}{\eta_2} + \frac{1}{\eta_2 + M_2}\right]\right) \end{aligned}$$

Thus,

$$\zeta^{\theta^*}(t) = -\left[\frac{\kappa^2}{2} + \lambda q \eta_2 \left(\frac{M_2}{\eta_2^2} - \frac{1}{\eta_2} + \frac{1}{\eta_2 + M_2}\right)\right] t + \kappa W(t) + \int_0^t \int_{\mathbb{R}^-} M_2 u \tilde{N}(ds, du).$$

Given an alternative measure Q^θ and the reference measure Q^0 , we can write the growth in entropy of Q^θ relative to Q^0 over the time interval $[t, t + \Delta t]$ as

$$G(t, t + \Delta t) = \mathbb{E}_t^\theta \left[\ln \left(\frac{Z^\theta(t + \Delta t)}{Z^\theta(t)} \right) \right], \quad \mathcal{R}(Z_t^\theta) = \lim_{\Delta t \rightarrow 0} \frac{G(t, t + \Delta t)}{\Delta t} \quad t \geq 0.$$

To calculate the above, it suffices to write $Z^\theta(t)$, especially $Z^{\theta^*}(t)$, under Q^θ or Q^{θ^*} . Using

Girsanov, we can write $Z^{\theta^*}(t)$ under Q^{θ^*} as

$$\begin{aligned}
dZ^{\theta^*}(t)/Z^{\theta^*}(t^-) &= \kappa(dW^{\theta^*}(t) + \kappa dt) - \int_{\mathbb{R}^-} (1 - e^{M_2 u})(\tilde{N}^{\theta^*}(dt, du) - (1 - e^{M_2 u})\nu(du)) \\
&= \left(\kappa^2 + \int_{\mathbb{R}^-} (1 - e^{M_2 u})^2 \nu(du) \right) dt + \kappa dW^{\theta^*}(t) - \int_{\mathbb{R}^-} (1 - e^{M_2 u}) \tilde{N}^{\theta^*}(dt, du) \\
&= \left(\kappa^2 + \int_{\mathbb{R}^-} (1 - 2e^{M_2 u} + e^{2M_2 u}) \lambda q \eta_2 e^{\eta_2 u} du \right) dt + \kappa dW^{\theta^*}(t) \\
&\quad - \int_{\mathbb{R}^-} (1 - e^{M_2 u}) \tilde{N}^{\theta^*}(dt, du) \\
&= \alpha_{\theta^*} dt + \kappa dW^{\theta^*}(t) - \int_{\mathbb{R}^-} (1 - e^{M_2 u}) \tilde{N}^{\theta^*}(dt, du)
\end{aligned}$$

with

$$\alpha_{\theta^*} = \kappa^2 + \lambda q \eta_2 \left(\frac{1}{\eta_2} - \frac{2}{\eta_2 + M_2} + \frac{1}{\eta_2 + 2M_2} \right),$$

and W^{θ^*} and $\tilde{N}^{\theta^*}(dt, du)$ being standard Brownian motion and compensated Poisson random measure under Q^{θ^*} . Here, $\tilde{N}^{\theta^*}(dt, du)$ has a Lévy measure $\nu^{\theta^*}(du)$ given by

$$\nu^{\theta^*}(du) = \lambda^* f_u^{\theta^*}$$

where

$$\begin{aligned}
\lambda^* &= \lambda(p + q\eta_2/(\eta_2 + M_2)) \\
f_u^{\theta^*} &= p^* \eta_1^* e^{-\eta_1^* u} 1_{u \geq 0} + q^* \eta_2^* e^{\eta_2^* u} 1_{u < 0},
\end{aligned}$$

where p^* , q^* , η_1^* , and η_2^* are defined in Proposition 3.

Hence, under Q^{θ^*} and by Itô formula, we have

$$\begin{aligned}
Z^{\theta^*}(t) &= \exp\left(\alpha_{\theta^*} t - \frac{\kappa^2 t}{2} + \kappa W^{\theta^*}(t) + \int_0^t \int_{\mathbb{R}^-} \ln(1 - (1 - e^{M_2 u})) \tilde{N}^{\theta^*}(ds, du)\right. \\
&\quad \left. + \int_0^t \int_{\mathbb{R}^-} [\ln(1 - (1 - e^{M_2 u})) + 1 - e^{M_2 u}] \nu^{\theta^*}(du)\right) \\
&= \exp\left(\left(\alpha_{\theta^*} - \frac{\kappa^2}{2}\right)t + \kappa W^{\theta^*}(t) + \int_0^t \int_{\mathbb{R}^-} [M_2 u + 1 - e^{M_2 u}] \lambda^* q^* \eta_2^* e^{\eta_2^* u} du\right. \\
&\quad \left. + \int_0^t \int_{\mathbb{R}^-} M_2 u \tilde{N}^{\theta^*}(ds, du)\right) \\
&= \exp\left(\alpha_{\theta^*}^* t + \kappa W^{\theta^*}(t) + \int_0^t \int_{\mathbb{R}^-} M_2 u \tilde{N}^{\theta^*}(ds, du)\right),
\end{aligned}$$

where

$$\alpha_{\theta^*}^* = \frac{1}{2}\kappa^2 + \lambda q \eta_2 \left(\frac{1}{\eta_2} - \frac{2}{\eta_2 + M_2} + \frac{1}{\eta_2 + 2M_2}\right) - \lambda^* q^* \eta_2^* \left(\frac{M_2}{(\eta_2^*)^2} - \frac{1}{\eta_2^*} + \frac{1}{\eta_2^* + M_2}\right).$$

Thus,

$$\ln\left(\frac{Z^{\theta^*}(t + \Delta t)}{Z^{\theta^*}(t)}\right) = \alpha_{\theta^*}^* \Delta t + \kappa \left(W^{\theta^*}(t + \Delta t) - W^{\theta^*}(t)\right) + \int_t^{t + \Delta t} \int_{\mathbb{R}^-} M_2 u \tilde{N}^{\theta^*}(ds, du).$$

$$G(t, t + \Delta t) = \mathbb{E}_t^{\theta^*} \left[\ln\left(\frac{Z^{\theta^*}(t + \Delta t)}{Z^{\theta^*}(t)}\right) \right] = \alpha_{\theta^*}^* \Delta t.$$

$$\mathcal{R}(Z_t^{\theta^*}) = \lim_{\Delta t \rightarrow 0} \frac{G(t, t + \Delta t)}{\Delta t} = \alpha_{\theta^*}^*.$$

Therefore, the constraint becomes

$$\mathcal{R}(Z_t^{\theta^*}) \leq h.$$

Here the value of h is to be determined by detection-error probabilities. For example, we set h such that the detection-error probability is at least 0.1. Furthermore, we can decompose $h = h_W + h_N$, meaning that we restrict the robustness concerns for drift ambiguity and jump ambiguity explicitly. In this regard, κ^* and M_2^* will depend on h_W and h_N , respectively.

C.3 Detection-error probabilities

The detection-error probability is defined as

$$\pi(t, n; h) = \frac{1}{2} \left[Q^0 \{ \zeta^{\theta^*}(n) > 0 | \mathcal{F}_t \} + Q^{\theta^*} \{ \zeta^{\theta^*}(n) < 0 | \mathcal{F}_t \} \right], \quad t \geq 0, n = mT,$$

where T is the number of years and m is the sampling frequency, and h denotes the upper bound for total robustness concern. Maenhout (2006) and Aït-Sahalia and Matthys (2019) provide a way to calculate this probability based on the characteristic functions of $\zeta^{\theta^*}(t)$ under Q^0 and Q^{θ^*} . That is

$$\pi(t, n; h) = \frac{1}{2} - \frac{1}{2\pi} \int_0^\infty \left(\Re \left[\frac{\phi_{\theta^*}(u, t, n)}{iu} \right] - \Re \left[\frac{\phi_0(u, t, n)}{iu} \right] \right) du,$$

where $i = \sqrt{-1}$ and $\Re(\cdot)$ denotes the real part of a complex number.

We can write $\phi_0(u, t, n) = \mathbb{E}_t [e^{iu\zeta^{\theta^*}(n)}]$ as

$$\begin{aligned} & E_t \left[\exp \left(iu(\alpha(n-t) + \kappa(W(n) - W(t)) + \int_t^n \int_{\mathbb{R}^-} M_2 v \tilde{N}(ds, dv) \right) \right) \\ &= \exp \left(iu\alpha(n-t) - \frac{\kappa^2 u^2}{2}(n-t) + (n-t) \int_{\mathbb{R}^-} (e^{iM_2 uv} - 1 - iM_2 uv) \nu(dv) \right) \\ &= \exp \left((n-t) \left[iu\alpha - \frac{\kappa^2 u^2}{2} + \int_{\mathbb{R}^-} (e^{iM_2 uv} - 1 - iM_2 uv) \lambda q \eta_2 e^{\eta_2 v} dv \right] \right) \\ &= \exp \left((n-t) \left[iu\alpha - \frac{\kappa^2 u^2}{2} + \lambda q \eta_2 \left(\frac{1}{iM_2 u + \eta_2} - \frac{1}{\eta_2} + \frac{iM_2 u}{\eta_2^2} \right) \right] \right), \end{aligned}$$

where

$$\alpha = - \left(\frac{\kappa^2}{2} + \lambda q \eta_2 \left[\frac{M_2}{\eta_2^2} - \frac{1}{\eta_2} + \frac{1}{\eta_2 + M_2} \right] \right).$$

For $\phi_{\theta^*}(u, t, n)$, we have $\phi_{\theta^*}(u, t, n) = \mathbb{E}_t^{\theta^*} [e^{iu\zeta^{\theta^*}(n)}] = \mathbb{E}_t [e^{iu\zeta^{\theta^*}(n)} e^{\zeta^{\theta^*}(n)}] = \mathbb{E}_t [e^{(iu+1)\zeta^{\theta^*}(n)}]$

as

$$\begin{aligned}
& \mathbb{E}_t \left[\exp \left((iu+1) \left[\alpha(n-t) + \kappa(W(n) - W(t)) + \int_t^n \int_{\mathbb{R}^-} M_2 v \tilde{N}(ds, dv) \right] \right) \right] \\
&= \exp \left((iu+1) \alpha(n-t) + \frac{(iu+1)^2 \kappa^2}{2} (n-t) \right) \mathbb{E}_t \left[\exp \left(\int_t^n \int_{\mathbb{R}^-} (iu+1) M_2 v \tilde{N}(ds, dv) \right) \right] \\
&= \exp \left((n-t) \left[(iu+1) \alpha + \frac{(iu+1)^2 \kappa^2}{2} + \int_{\mathbb{R}^-} \left(e^{(iu+1)M_2 v} - 1 - (iu+1)M_2 v \right) \nu(dv) \right] \right) \\
&= \exp \left((n-t) \left[(iu+1) \alpha + \frac{(iu+1)^2 \kappa^2}{2} + \int_{\mathbb{R}^-} \left(e^{(iu+1)M_2 v} - 1 - (iu+1)M_2 v \right) \lambda q \eta_2 e^{\eta_2 v} dv \right] \right) \\
&= \exp \left((n-t) \left[(iu+1) \alpha + \frac{(iu+1)^2 \kappa^2}{2} + \lambda q \eta_2 \left(\frac{1}{(iu+1)M_2 + \eta_2} - \frac{1}{\eta_2} + \frac{(iu+1)M_2}{\eta_2^2} \right) \right] \right)
\end{aligned}$$